Response to Anonymous Referee #1

We thank the reviewer for the constructive suggestions/comments. Below we provide a point-by-point response to individual comments (comments in italics, responses in plain font; page numbers refer to the ACPD version; figures used in the response are labeled as Fig. R1, Fig. R2,…).

Comments and suggestions:

NO2 measurement: MAX-DOAS measures slant column densities which were converted to vertical column densities as described in line 157 to 162. The authors describe how they convert a vertical column density to local NO2 concentrations in the Supplement. They assume homogeneous concentrations within a 500 m thick boundary layer (BL) irrespective of daytime. Constant height of a boundary layer (BL) over a daytime is not realistic and will deliver a false diurnal variation of NO2 concentrations. Neither is a constant height of BL of 500 m applicable to different seasons.

Responses and Revisions:

Differential Optical Absorption Spectroscopy (DOAS) is used to retrieve NO_2 and O_4 differential slant column densities (DSCDs) from the measured scattered sunlight spectra (Platt, 1994). In this study, each MAX-DOAS scanning cycle consists of eight elevation viewing angles (2 °, 3 °, 6 °, 8 °, 10 °, 20 °, 30 °and 90 °) and lasts about 15 min. The spectra are analyzed using the QDOAS spectral-fitting software suite developed at BIRA-IASB (http://uv-vis.aeronomie.be/software/QDOAS/). Detail information about the spectral fitting for NO_2 and O_4 is listed in Table S2 (in the revised supplement). As pointed out by the reviewer, MAX-DOAS vertical column densities could not fully represent the NO_2 surface concentration. So we used the HEIPRO (Heidelberg Profile,

样式定义：EndNote Bibliography: (中文) 中文(中国), (其他) 英语(美国), 行距：单倍行距

带格式的：中文(中国)

developed by IUP Heidelberg) retrieval algorithm to retrieve NO_2 vertical profiles for each MAX-DOAS scanning cycle. The purpose of calculating NO_2 profiles is to know the NO_2 vertical distribution. More details about NO_2 profile retrieval are described in the revised supplement. The NO_2 vertical profile was shown in Fig. R1, indicating that the NO_2 is not homogeneously distributed vertically. We agree with the reviewer that converting NO_2 $DSCD_S$ to mixing ratios by assuming that the trace gases were homogeneous within the 500 m height of the boundary is not suitable. We took the suggestion from the reviewer and updated the NO_2 results in the revision. The retrieval altitude grid is 80 layers of 50m thickness between 0.02 and 3.97 km. Thus, in the revised manuscript we have revised our method by using the surface NO_2 concentration (0.02 km) which from the NO_2 vertical profile (Fig. R1) to analyze. Due to the large computational requirement, we were not able to complete the calculation of the NO2 vertical profile for the whole year. However, in Figure R1 we showed the result of one such NO2 vertical profile (20th November, 2013), and the DFS and the errors of the retrieval are to determine whether the retrieved method is reasonable or not. As shown in Figure R2, the results suggest that the retrieved NO_2 vertical profile is reliable according to the experience of other research (Wang et al., 2014).

带格式的：中文(中国)

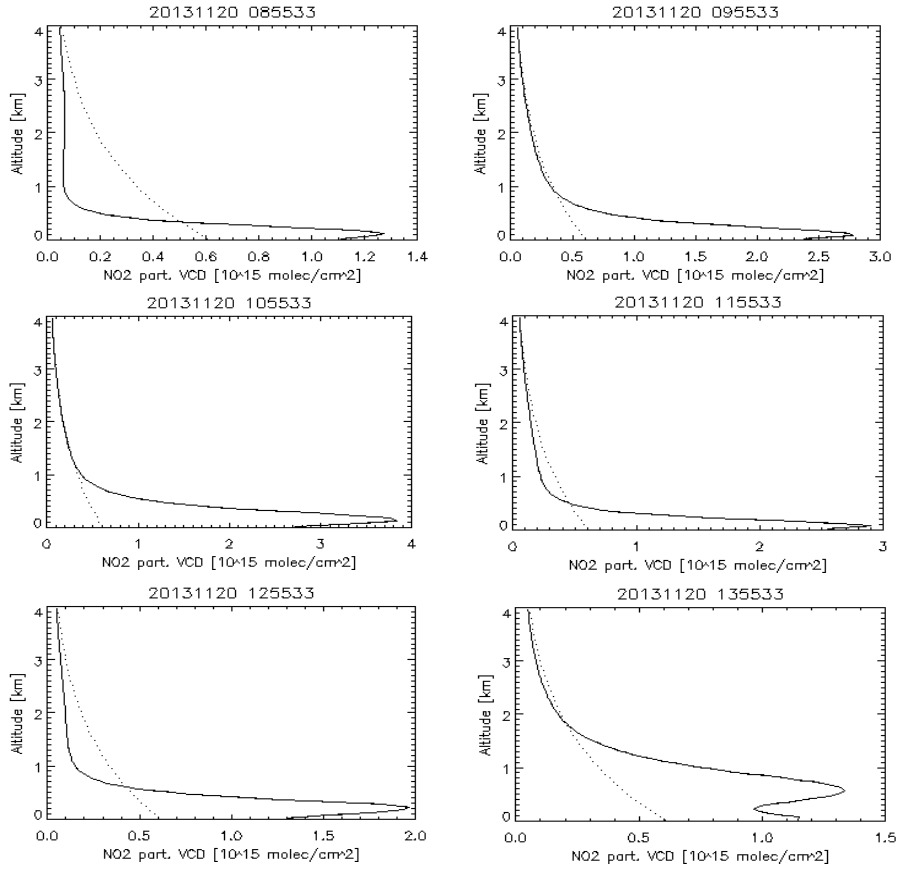

Figure R1. Example NO_2 vertical profiles at six different times (shown on top of each graph as YYYYMMDD hhmmss) from MAX-DOAS measurements in Hefei (20 November, 2013).

带格式的：中文(中国)

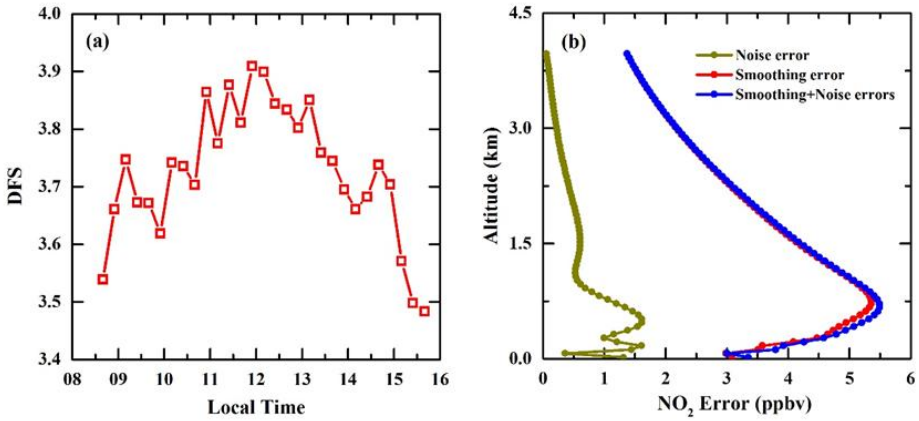

Figure R2. (a) DFS diurnal cycles corresponding to the NO2 profile retrievals; (b) Errors of NO2 vertical profile retrieval from MAX-DOAS measurements at Hefei (20 November, 2013 at 10:25LT).

Comments and suggestions:

Section 4.1: The discussion of the PSCF results is difficult to follow. Figure 5 shows potential source areas of GEM during the haze events in December 2013 and January 2014 but the equivalent figures for non-haze days in December 2013 and January 2014 are shown only in supplementary information. It is their difference which can provide the information about the reason for higher GEM during the hazy days. Dtto about the Figure 6: two seasonal data sets should be presented, one for hazy days and one for non-hazy ones.

Responses and Revisions:

We have updated and merged PSCF results for potential source areas analysis of GEM in the revised manuscript. Two seasonal data sets are now include, one for haze days and the one for non-haze days. Since the number of haze days accounts only for 5.6% of the total days in spring and summer, we did not provide haze and non-haze PSCF results for spring and summer seasons. As autumn and winter are the prevalent

带格式的：中文(中国)

seasons for haze pollution, one PSCF result for haze days and another for non-haze days are shown for autumn and winter, respectively. We have combined Figure 5 and Figure 6 into a new figure (Figure 4) in the revised manuscript. The updated PSCF results showed that higher GEM concentration was mainly influenced by local emission sources during haze days. For non-haze days, the most important mercury sources to the monitoring site were not only the local emission sources, but also those from the neighboring region of Shandong, Henan and Jiangxi provinces. In summary, the increase of GEM concentration during haze days was mainly caused by local emission.

Comments and suggestions:

The discussion of GEM vs CO correlations is deeply flawed. The low GEM/CO slopes are interpreted as if biomass burning were the major source for both GEM and CO in Hefei. To start with GEM/CO slopes represent their emission ratios if a) the background concentrations do not change, b) the emissions remain constant, and c) there is only dilution, no chemistry, on the way from the source to receptor during an event. Using monthly or other "non-event" data would violate at least the condition a) and b). In addition, whatever the sources of GEM might be, in a city of 7 million people and some 1 million of vehicles most of the CO at the site within the city will almost certainly come from local tailpipes rather than from distant isolated fire counts shown in Figure S4. The authors present Figure S3 as additional evidence in favour of biomass burning being the major source. The figure shows correlation between K+ and an Air Quality Index, whose definition is not given in the paper. To be halfway credible, K+ has to be correlated with CO. Even if K+ correlated with CO, it still will not prove the biomass burning origin of the mercury. For that the density of the fire counts has to

带格式的：中文(中国)

be consistent with results of the PSCF analysis which it evidently is not. In addition remote biomass burning would not yield highest GEM, RGM, and PBM concentration at the lowest wind speeds-see section 4.2. In summary, the low GEM/CO ratio is characteristic for the emissions of Hefei.

Responses and Revisions:

Upon further examination of our data, we agree with the reviewer that our original interpretation of the low GEM/CO was not fully supported. Therefore, we have removed Figure S2 (in the ACPD supplement) and revised thoroughly section 4.1 regarding the GEM/CO ratio. The definition of mercury pollution events are not same as haze days in this paper. These mercury pollution episodes were defined as a period with hourly average GEM concentration higher than seasonal average GEM concentration and the duration of elevated hourly GEM concentration lasted for over 10 hours (Kim et al., 2009). We discussed the correlation coefficients and slopes between GEM concentration and CO concentration during pollution events (Table 3 in the revised manuscript). In previous research, the Hg/CO slope and correlation between GEM and CO concentrations has been used to identify long-range transport episodes or local episodes: significant positive correlation for long-range transport episodes and poor correlation for local episodes (Kim et al., 2009). According to the correlations between GEM concentration and CO concentration, the mercury pollution episodes in autumn and winter mainly belong to local episodes. Incomplete combustion like residential coal and biomass burning combustion could lead to a lower Hg/CO ratio. We agree with the reviewer's point. In summary, the low GEM/CO ratio may be characteristic for the local emissions of Hefei.

带格式的：中文(中国)

As for water-soluble potassium (K^+) in 24-hr PM_{10} samples, the correlation between K^+ and Air Quality Index maybe not reliable. So we did the correlation between K^+ and GEM during the 24-hr PM_{10} sampling period (Fig. R3). Although the concentration of water-soluble potassium (K^+) in PM_{10} shows a good correlation (R^2=0.67) with GEM, due to the small number of compared samples (n=6), so it has great accidental and uncertainty. In addition, most pollutant concentration increased during this heavy pollution episodes (Nov-Dec, 2013). Good correlation might occur between K+ and other pollutant, so it cannot fully prove that GEM come from the emission of biomass burning through good correlation between K^+ and GEM. Thus, we agree with the reviewer's comment and shortening this section. We have removed the discussion about K^+ and biomass burning altogether in the revised manuscript and supplement.

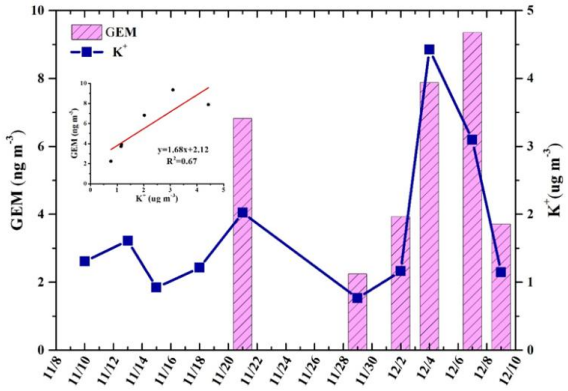

Figure R3. Correlation between water-soluble potassium (K+) and GEM during heavy pollution periods (from 10 Nov to 9 Dec, 2013). Notes: water-soluble potassium (K^+) concentrations were analyzed from 24-hr PM_{10} (particulate matter less than 10 μm in diameter) samples, GEM concentrations were the average value during the 24-hr PM_{10} sampling period.

带格式的：中文(中国)

Comments and suggestions:

Section 4.2: Highest PBM and PM2.5 concentrations in January are most likely due to shallower boundary layer in January than in other months. That is probably meant by "poor diffusion conditions in cold months". The average PBM concentrations in March differ hardly from other months except for January but their spread is larger. I think that the precipitation and the frequency of change of air masses should be also taken into account as driving forces for the PBM vs PM2.5 correlation.

Responses and Revisions:

We agree with the reviewer's suggestion. Unfortunately, we did not obtain the precipitation data during our monitoring period, so we were not able to directly examine the influence of precipitation on PBM. This is something we will investigate in our future studies.

Although on average the PBM concentrations in March differ hardly from other months (April-June), they fluctuated much greatly in March when compared to other months. We have re-examined the wind rose diagrams for March and April (see Fig. R4). The prevailing wind direction in March indeed varied much greatly than in April. Thus, the larger fluctuation of PBM in March might be related to the frequency of change in wind direction. We have thus removed our original interpretation that "higher temperatures in the warmer months do not favor mercury adsorption", and replaced it with reference to changes in wind direction.

带格式的：中文(中国)

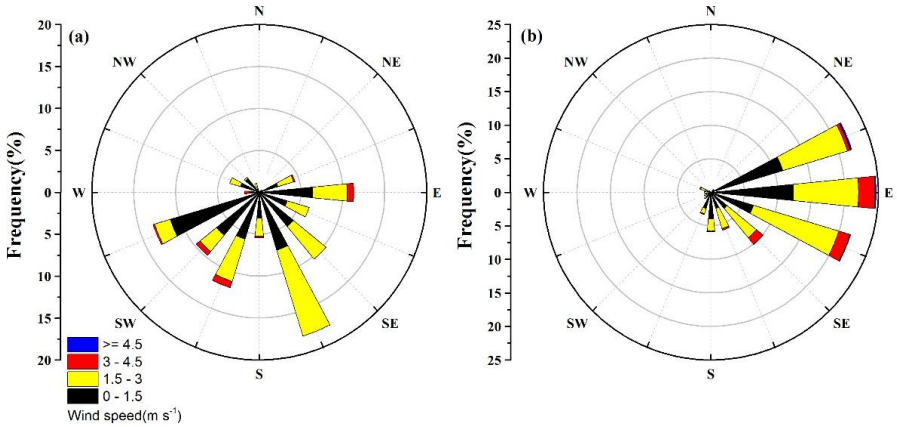

Figure R4. The wind rose diagrams for (a) March and (b) April.

Comments and suggestions:

Section 4.3: The interpretation of the diurnal variations here is almost certainly wrong. The authors interpret GEM and PBM diurnal variation in terms of changing height of boundary layer and declare that the opposite RGM diurnal variation must be of chemical origin. This must not be and probably is not true. RGM correlates with O3 which is probably not formed in situ but admixed from the free troposphere (FT) as the height of BL increases during the morning. Higher RGM concentrations in FT than in BL have been reported by many researchers. Consequently, the RGM correlation with O3 and its anticorrelation with CO can be viewed as solely a transport phenomenon unrelated to any chemical process. The distinction between a transport and chemical processes is a general problem in the interpretation of diurnal variations. It can only be resolved by careful modeling using measured diurnal variation of the BL height and known concentrations in BL and FT or by using specific tracers for photochemical processes such as peroxynitrites. In this particular case, diurnal variations of GEM, PBM, CO, NOx, etc. emissions due to morning and evening rush hours, working times, etc. additionally complicate the interpretation of the diurnal variations. As mentioned

带格式的：中文(中国)

before the diurnal variation of NO2 is also flawed by the assumption of constant height of boundary layer. In summary, the observed diurnal variation can be interpreted solely as a transport phenomenon due to air exchange between BL and FT. As long as the authors cannot rule out the transport hypothesis their chemical interpretation of the diurnal variation and discussion of NO2 kinetics are wishful thinking without any evidential basis.

Responses and Revisions:

We agree with the reviewer that resolving transport and reaction processes of RGM is not straightforward; the fact that we did not measure specific photochemical tracers such as peroxynitrites did not help. Two processes can affect the RGM concentrations in the boundary layer air. The first is due to transport of RGM from the free troposphere (FT). Diurnal variations of GEM, RGM, O_3 and CO concentrations during non-haze and haze days are shown in Fig. R5 (Figure 7 in the revised manuscript). For both non-haze and haze days, RGM concentrations remained at a relatively constant level during night, and then increased suddenly prior to the sunrise. We agree with the reviewer that such enhancement of RGM in early morning might can be due, at least in part, to its transport from the free troposphere as the height of BL increases. In summary, the observed RGM diurnal variation can be interpreted as a transport phenomenon due to air exchange between BL and FT.

In addition, in situ photochemical oxidation of GEM could also increase the concentration of RGM during daytime. To determine the relative importance of FT transport and in situ photochemical oxidation, we examined the relationship between RGM and the changes in the height of the atmospheric boundary layer and the odd oxygen (O_X= O_3+NO_2) concentrations. Although we did not measure peroxynitritesin

带格式的：中文(中国)

this study, we believe the concentration of odd oxygen (O_X = O_3+NO_2 which is produced from the reaction between O3 and NO) can be used as a tracer of the extent of photochemical processing in the urban atmosphere. Since NO_2 concentrations from MAX-DOAS were only available during daytime, we could only use O_X to be a indicator for daytime GEM oxidation. As per our manuscript, we selected 20th November 2013 as a case study to probe the importance of photochemical processes. Both RGM and O_X reached higher concentrations from 12:00 to 16:00, along with the lowest value of GEM. The height of atmospheric boundary layer changed very little over this period (12:00-16:00, see Fig. R6). This simple comparison suggests that the transport of FT RGM might be limited and that at least some of the RGM were formed from in situ oxidation of GEM. We further investiagted the potential mechanism of the GEM oxidation to GOM.

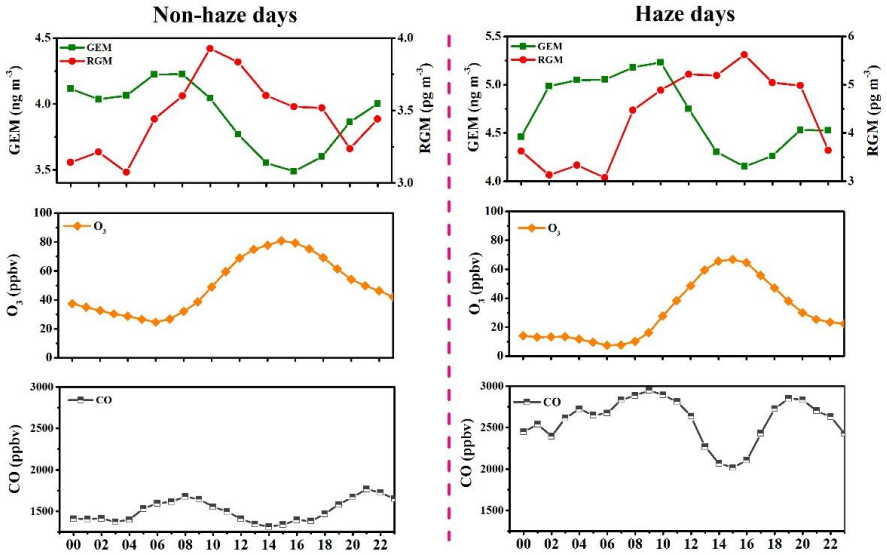

Figure R5. Diurnal variations of GEM, RGM, O_3, and CO concentrations during non-haze and haze days.

带格式的：中文(中国)

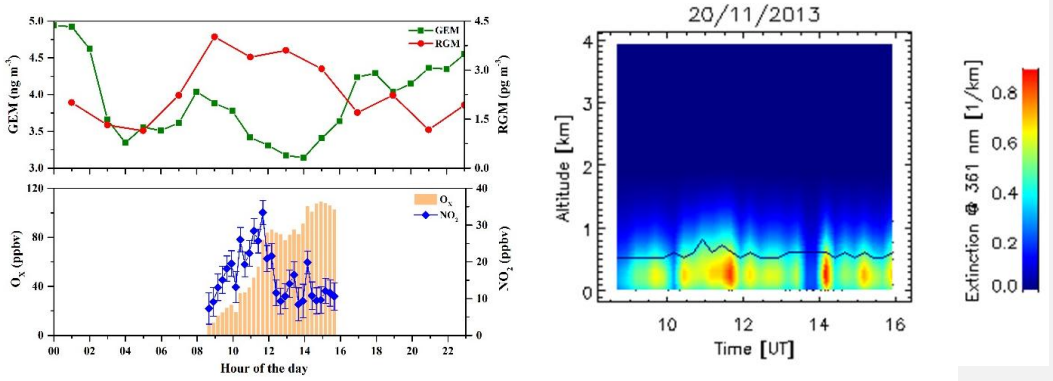

Figure R6. A case study of diurnal variations of GEM, RGM, O_X, and NO_2 at Hefei (20th November, 2013, left panel). The right panel shows the retrieved aerosol extinction profile on the same day; the black line represents the height of the atmospheric boundary layer.

Comments and suggestions:

Line 66-67: PBM is not highly surface reactive. "Affinity" might be better than "reactivity".

Responses and Revisions:

Corrected.

Comments and suggestions:

Line 72: The most recent quoted reference is Pacyna et al. (2006). In 2016 and recent discussions about emissions this seems to be quite obsolete. Dtto line 82. Please quote more recent publications.

Responses and Revisions:

We have updated the section by quoting two recent publications ((Pacyna et al., 2010) and (Zhang et al., 2015)).

Comments and suggestions:

Line 322: The sentence is flawed both in content as in grammar. If taken at face value, the text insinuates emissions from power plants being "non-normal" although

带格式的：中文(中国)

they represent the largest GEM emissions in most inventories. Reference at line 584 is incomplete.

Responses and Revisions:

The sentence in Line 322 has been modified according to the revision in the revised manuscript (second paragraph of section 4.1). We modified this sentence as follows: "GEM and CO often share similar anthropogenic emission sources, such as industrial coal combustion, domestic coal combustion, iron and steel production and cement production (Wu et al., 2006;Wang et al., 2005). However, they also have their own sources. For instance, power plants and nonferrous metal smelters emit mercury but hardly any CO, while most of CO originates from vehicles which are not a major emitter for mercury."

We also corrected the reference at line 584 (Hu et al., 2014).

Comments and suggestions:

Figure 8: Bottom plot: which symbol is PBM and which one PM2.5? The caption of the Figure 8 seems to be inconsistent with the time scale of the bottom plot. The time scale of the bottom plot has not equidistant intervals.

Responses and Revisions:

We have rearranged the figures, added the symbols of PBM and $PM_{2.5}$ and updated the caption. The time scale of the bottom plot has corrected and had equidistant intervals.

Comments and suggestions:

Figure 9: The scales of the y-axes should be same for the haze and non-haze days to facilitate a comparison. E.g. CO mixing ratios are much higher on hazy days.

Responses and Revisions:

带格式的：中文(中国)

We have redrawn the figures so that the scales of the y-axes are same for the haze and non-haze days.

References

Kim, S. H., Han, Y. J., Holsen, T. M., and Yi, S. M.: Characteristics of atmospheric speciated mercury concentrations (TGM, Hg(II) and Hg(p)) in Seoul, Korea, Atmospheric Environment, 43, 3267-3274, doi:10.1016/j.atmosenv.2009.02.038, 2009.

Pacyna, E. G., Pacyna, J., Sundseth, K., Munthe, J., Kindbom, K., Wilson, S., Steenhuisen, F., and Maxson, P.: Global emission of mercury to the atmosphere from anthropogenic sources in 2005 and projections to 2020, Atmospheric Environment, 44, 2487-2499, 2010.

Platt, U.: Differential optical absorption spectroscopy (DOAS), Air monitoring by spectroscopic technique, 127, 27-84, 1994.

Wang, L., Zhang, Q., Hao, J., and He, K.: Anthropogenic CO emission inventory of Mainland China, Acta Scientiae Circumstantiae, 25, 1580-1585, 2005.

Wang, T., Hendrick, F., Wang, P., Tang, G., Clémer, K., Yu, H., Fayt, C., Hermans, C., Gielen, C., and Müller, J.-F.: Evaluation of tropospheric SO_2 retrieved from MAX-DOAS measurements in Xianghe, China, Atmospheric Chemistry and Physics, 14, 11149-11164, 2014.

Wu, Y., Wang, S., Streets, D. G., Hao, J., Chan, M., and Jiang, J.: Trends in anthropogenic mercury emissions in China from 1995 to 2003, Environmental science & technology, 40, 5312-5318, 2006.

Zhang, L., Wang, S., Wang, L., Wu, Y., Duan, L., Wu, Q., Wang, F., Yang, M., Yang, H., and Hao, J.: Updated Emission Inventories for Speciated Atmospheric Mercury from Anthropogenic Sources in China, Environmental science & technology, 49, 3185-3194, 2015.

带格式的：中文(中国)

Response to Anonymous Referee #2

We thank the reviewer for the constructive suggestions/comments. Below we provide a point-by-point response to individual comments (comments in italics, responses in plain font; page numbers refer to the ACPD version; figures used in the response are labeled as Fig. R1, Fig. R2,…).

Comments and suggestions:

Minor issues Line 40: "and" should be placed between "spring, summer".

Responses and Revisions:

Corrected.

Comments and suggestions:

Line 55 and all other lines: Several years ago, the atmospheric mercury community stopped using the term "reactive gaseous mercury". This term was replaced with "GOM", gaseous oxidized mercury. I suggest you change all of your RGM to GOM.

Responses and Revisions:

Agreed and corrections have been made in the text and figures.

Comments and suggestions:

Line 148: change "limits" to "limit".

Responses and Revisions:

Corrected.

Comments and suggestions:

Line 187: you mentioned an arbitrarily set criterion of 4 ng m-3. I really don't know much about PSCF, but why do you use arbitrary criteria. How will different arbitrary criteria affect your results?

Responses and Revisions:

带格式的：中文(中国)

The "arbitrarily set criterion" was used in the definition of M_{ij} in the PSCF analysis (see TrajStat_Help_v1.2). The definition of M_{ij} as follows: The number of endpoints for the same cell having arrival times at the sampling site corresponding to pollutant concentration higher than an arbitrarily set criterion is defined to be M_{ij}. In this study, pollutant concentration refers to atmospheric mercury concentration (GEM concentration). The words "arbitrarily set criterion" were used in PSCF method introduction and could also be found in (Fu et al., 2012). However, in the actual operation, we use a fixed GEM value as criterion. In this study, mean GEM concentration of 4 ng m^{-3} during the whole study period was used as fixed criterion (refer to Fu et al., 2012). We split the sentence in Lines 192-195 (ACPD version) to describe clearly in the revised manuscript.

Comments and suggestions:

Line 241: "folds" should be fold or two-fold.

Responses and Revisions:

Corrected

Comments and suggestions:

Line 296: change "sources region" to "source region".

Responses and Revisions:

Corrected.

Comments and suggestions:

Line 333: change "condition" to "conditions".

Responses and Revisions:

Corrected.

Comments and suggestions:

带格式的：中文(中国)

Line 391: remove (and) from you reference (Sommar et al. 2001).

Responses and Revisions:

Corrected

Comments and suggestions:

Line 454: change "may plays" to "may play"

Responses and Revisions:

Corrected.

Comments and suggestions:

Line 456: change "greatly" to "great"

Responses and Revisions:

Corrected.

Comments and suggestions:

Table 2 should be updated to include mercury speciation studies conducted in the US over the past few years. There are several studies in the peer-reviewed literature that can be cited in this table, bring it up to date.

Responses and Revisions:

Agreed. We have added (Peterson et al., 2012) and (Ren et al., 2016) in Table 2.

Comments and suggestions:

Figure 3. Can you eliminate this figure? These data on already in Table 1.

Responses and Revisions:

We assume the reviewer meant Figure 4 in the ACPD version. The only overlap of data between this figure and Table 1 are GEM, RGM and PBM mean concentrations. This figure also provides further information such as various percentiles. We agree with the reviewer's comment and move this figure into the supplement.

Comments and suggestions:

带格式的：中文(中国)

Figures 4 and 5. Can you merge these two figures into a single figure?

Responses and Revisions:

We assume the reviewer meant Figures 5 and 6. We have merged PSCF results for potential source areas analysis of GEM in the revised manuscript. Two seasonal data sets have presented, one for haze days and another one for non-haze days.

References

Fu, X. W., Feng, X., Shang, L. H., Wang, S. F., and Zhang, H.: Two years of measurements of atmospheric total gaseous mercury (TGM) at a remote site in Mt. Changbai area, Northeastern China, Atmospheric Chemistry and Physics, 12, 4215-4226, doi:10.5194/acp-12-4215-2012, 2012.

Peterson, C., Alishahi, M., and Gustin, M. S.: Testing the use of passive sampling systems for understanding air mercury concentrations and dry deposition across Florida, USA, Science of the Total Environment, 424, 297-307, 2012.

Ren, X., Luke, W. T., Kelley, P., Cohen, M. D., Artz, R., Olson, M. L., Schmeltz, D., Goldberg, D. L., Ring, A., and Mazzuca, G. M.: Atmospheric mercury measurements at a suburban site in the Mid-Atlantic United States: Inter-annual, seasonal and diurnal variations and source-receptor relationships, Atmospheric Environment, 2016.

带格式的：中文(中国)

Speciated Atmospheric Mercury during Haze and Non-haze Days in an Inland City in China

Qianqian Hong[1,3], Zhouqing Xie[1,2,3*], Cheng Liu[1,2,3*], Feiyue Wang[4], Pinhua Xie[2,3], Hui Kang[1], Jin Xu[2], Jiancheng Wang[1], Fengcheng Wu[2], Pengzhen He[1], Fusheng Mou[2], Shidong Fan[1], Yunsheng Dong[2], Haicong Zhan[1], Xiawei Yu[1], Xiyuan Chi[1], Jianguo Liu[2]

1. School of Earth and Space Sciences, University of Science and Technology of China, Hefei, 230026, China

2. ~~Innovation~~CAS Center for Excellence in ~~Urban~~Regional Atmospheric Environment ~~of CAS~~ & Institute of Urban Environment of CAS, Xiamen, 361021, China

3. Key Lab of Environmental Optics ~~&~~and Technology, Anhui Institute of Optics and Fine Mechanics, Chinese Academy of Sciences, Hefei, 230031, China

4. Centre for Earth Observation Science, and Department of Environment and Geography, University of Manitoba, Winnipeg, MB R3T 2N2, Canada

Correspondence author:

zqxie@ustc.edu.cn (Z.Q.X.); chliu81@ustc.edu.cn (C.L.)

带格式的：字体颜色：自动设置

带格式的：字体颜色：自动设置，英语(美国)

带格式的：字体颜色：自动设置

带格式的：字体颜色：自动设置

带格式的：字体颜色：自动设置

带格式的：字体颜色：自动设置

带格式的：字体颜色：自动设置

带格式的：字体颜色：自动设置

带格式的：字体颜色：自动设置

带格式的：字体颜色：自动设置

带格式的：字体颜色：自动设置

带格式的：字体颜色：自动设置

带格式的：字体颜色：自动设置

带格式的：字体颜色：自动设置

带格式的：中文(中国)

Abstract. Long-term continuous measurements of speciated atmospheric mercury were conducted from July 2013 to June 2014 at Hefei, a mid-latitude inland city in east central China~~, from July 2013 to June 2014.~~ that experiences frequent haze pollution. The mean concentrations (±standard deviation) of gaseous elemental mercury (GEM), ~~reactive~~ gaseous oxidized mercury (~~RGM~~GOM) and particle-bound mercury (PBM) were 3.95 ± 1.93 ng m^{-3}, 2.49 ± 2.41 pg m^{-3} and 23.3 ± 90.8 pg m^{-3}, respectively, during non-haze days, and 4.74 ±1.62 ng m^{-3}, 4.32 ± 8.36 pg m^{-3} and 60.2 ± 131.4 pg m^{-3}, respectively, during haze days. Potential source contribution function (PSCF) analysis suggested that the atmospheric mercury pollution during haze days was caused primarily by local mercury emissions, instead of via long-range mercury transport. ~~In addition, the~~ The disadvantageous ~~diffussion~~diffusion during haze days ~~will~~ also ~~enhance~~favoured the ~~level~~accumulation of atmospheric mercury. Compared to ~~the~~ GEM and ~~RGM, change in~~GOM, PBM was found to be more sensitive to ~~the~~ haze pollution. The mean PBM concentration during haze days was 2.5 times that during non-haze days due to elevated concentrations of particulate matter. A remarkable seasonal trend in PBM was also observed with concentration decreasing in the following order in response to the frequency of haze days: autumn, winter, spring~~,~~ and summer. ~~A distinct~~For both non-haze and haze days, GOM concentrations remained at relatively constant during night, but increased rapidly prior to sunrise. This GOM diurnal ~~relationship was found~~variation could be due to diurnal variation in air exchange between ~~GEM and RGM during haze days, with the peak values of RGM coinciding with~~boundary layer and free troposphere, but the ~~decline in GEM. Using HgOH as an intermediate product during GEM~~contribution from photochemical oxidation~~, our~~ could not be ruled out. This is supported by simple

带格式的：字体颜色：自动设置
带格式的：字体颜色：自动设置
带格式的：字体颜色：自动设置
带格式的：字体颜色：自动设置
带格式的：字体颜色：自动设置
带格式的：字体颜色：自动设置
带格式的：字体颜色：自动设置
带格式的：字体颜色：自动设置
带格式的：字体颜色：自动设置
带格式的：字体颜色：自动设置
带格式的：字体颜色：自动设置
带格式的：字体颜色：自动设置
带格式的：字体颜色：自动设置
带格式的：字体颜色：红色
带格式的：字体颜色：红色
带格式的：字体颜色：红色
带格式的：字体颜色：红色
带格式的：中文(中国)

box-model calculations, which showed that oxidation of GEM to GOM does occur and that the transport of free troposphere GOM alone is not large enough to account for the observed increase in GOM. Our results ~~suggest~~postulate that NO_2 aggregation with ~~HgOH could explain~~the HgOH intermediate may be a potential mechanism for the enhanced production of ~~RGM~~GOM during ~~the~~ daytime ~~in haze days. Increasing level of NOx will potentially accelerate the oxidation of GEM despite the decrease of solar radiation~~.

1. Introduction

Mercury (Hg) is an environmental pollutant that has received much global attention because of its toxicity and bioaccumulation via the aquatic food chain. The most important transport pathway of mercury is via the atmosphere ~~(Schroeder and Munthe, 1998~~(Schroeder and Munthe, 1998;Lindqvist and Rodhe, 1985). Operationally, atmospheric mercury is commonly differentiated into three forms: gaseous elemental mercury (GEM), ~~reactive~~ gaseous oxidized mercury (~~RGM~~GOM) and particle-bound mercury (PBM). The sum of these three atmospheric speciated mercury is defined as total atmospheric mercury (TAM = GEM + ~~RGM~~GOM + PBM), and the sum of GEM and ~~RGM~~GOM is known as total gaseous mercury (TGM = GEM + ~~RGM~~GOM) ~~(Gustin and Jaffe, 2010;Gustin et al., 2015)~~(Gustin and Jaffe, 2010;Gustin et al., 2015). GEM is regarded as the ~~predominant~~dominant form of atmospheric mercury, accounting for over 95% of the total. GEM is stable in the ~~atmosphere~~troposphere with a long residence time (0.5–2 yr) and can be transported at the regional to global scale ~~(Schroeder and Munthe, 1998;Lindberg et al.,~~

带格式的：字体颜色：红色
带格式的：字体颜色：红色
带格式的：字体颜色：红色
带格式的：字体颜色：红色
带格式的：字体颜色：红色
带格式的：字体颜色：红色
带格式的：字体颜色：自动设置
带格式的：行距：1.5 倍行距
带格式的：字体颜色：红色
带格式的：字体颜色：红色
带格式的：字体颜色：红色
带格式的：字体颜色：自动设置
带格式的：字体颜色：自动设置
带格式的：字体颜色：自动设置
带格式的：字体颜色：自动设置
带格式的：字体颜色：自动设置
带格式的：字体颜色：自动设置
带格式的：中文(中国)

2007)(Schroeder and Munthe, 1998;Lindberg et al., 2007). GEM can be oxidized to RGM through photochemical processes, and further transformed to PBM on aerosol surfaces. Although GEM is the predominant form of mercury in the air, trace amounts of RGM and PBM control the mercury scavenged from the atmosphere (Lindberg and Stratton, 1998). RGM. GEM can be oxidized to GOM through photochemical processes, and further transformed to PBM on aerosol surfaces. GOM and PBM can be readily removed form the air by wet and dry deposition as a result of their high surface reactivityaffinity and water solubility (Lindqvist and Rodhe, 1985). Thus, the chemical transformationstransformation between GEM, RGMGOM and PBM will directly influence the atmospheric lifetime of mercury.

As a result of the rapid industrial development and economic growth of recent decades, China has become one of the major contributors to anthropogenic mercury emissions to the environment (Wu et al., 2006;Pacyna et al., 2006;Streets et al., 2005)(Wu et al., 2006;Pacyna et al., 2006;Pacyna et al., 2010;Zhang et al., 2015b). Atmospheric mercury emissions from anthropogenic sources in China have been estimated to be in the range of 500-700 tons/yr, accounting for 25-30% of the total global anthropogenic mercury emissions (Streets et al., 2005;Wu et al., 2006)(Streets et al., 2005;Wu et al., 2006). Research into atmospheric mercury in China is therefore critical to the understanding of mercury cycling at both regional and global scales. Long-term observation of atmospheric mercury has been conducted in different regions in China, including both urban and remote areas. TGM concentrations observed in urban and industrial regions of China were in the range of 2.7–35 ng m^{-3}, higher than the values reported for North America and Europe, and for the adjacent Asian countries such as Korea and Japan (Stamenkovic et al., 2007;Dommergue et al.,

带格式的：字体颜色：自动设置

带格式的：字体颜色：自动设置

带格式的：字体颜色：自动设置

带格式的：字体颜色：自动设置

带格式的：字体颜色：红色

带格式的：字体颜色：自动设置

带格式的：中文(中国)

2002;Fang et al., 2009)(Weigelt et al., 2013;Fang et al., 2009;Marumoto et al., 2015). TGM and PBM concentrations in remote areas of China were also found to be higher than those observed in North America and Europe (Fu et al., 2008a;Fu et al., 2008b;Fu et al., 2012(Fu et al., 2008a;Fu et al., 2008b;Fu et al., 2012;Liu et al., 2010).

In recent years, haze pollution has become a major concern in China due to its impacts on visibility, air quality, and climate. It is well known that haze formation is mainly dependent on the atmospheric relative humidity (RH) and the concentration of airborne particles (Chen et al., 2003;Sun et al., 2013);Sun et al., 2013). Most studies on haze have focused on the measurements of airborne particulate matter; few examined the influence of haze on the chemistry of atmospheric mercury, especially PBM. In this study, we conducted one year synchronous observations of speciated atmospheric mercury in Hefei, an inland city of China, which experiences frequent haze events. The comparision of atmospheric mercury under haze days and non-haze days during the study period allows us to examine the formation and deposition mechanisms of mercury, as well as their temporal variations.

2. Methods

2.1 Study site

Continuous measurements of speciated atmospheric mercury were undertaken in Hefei (31°52′ N, 117°17′ E) from July 2013 to June 2014. Hefei, the capital of Anhui Province, is located in east central China, between the Changjiang (Yangtze River) and the Huaihe (Huai River). Hefei has a humid subtropical climate with four distinct seasons: June-August is considered summer, September-November autumn, December-February winter and March-May spring. The prevailing wind is

带格式的：字体颜色：自动设置

带格式的：中文(中国)

southeasterly in summer and northwesterly in winter. Like many Chinese cities, Hefei has experienced rapid growth in the past 20 years. The total permanent population is about 7.7 million. The city has also been witnessing an increasing frequency in haze pollution, especially in winter months.

The monitoring site was located on the Science Island, a small peninsula on the Dongpu Reservoir in the northwestern outskirts of Hefei (Fig. 1). The sampling and analytical instruments were installed 1.5 m above the rooftop (~ 20 m above the ground) of the main building of Anhui Institute of Optics and Fine Mechanics. Further information about the monitoring site can be found in a previous study ~~(Hu et al., 2014)~~(Hu et al., 2014). We chose this area as the monitoring site because it is one of the cleanest areas in Hefei, not adjacent to any direct pollution sources such as power plants, iron and steel works.

2.2 Measurements of speciated atmospheric mercury

From July 2013 to June 2014, simultaneous measurements of speciated atmospheric mercury concentrations were performed by an automated Tekran™ mercury speciation system. The system consisted of a Model 2537B mercury analyzer combined with a Model 1130 ~~RGM~~GOM unit and a Model 1135 PBM unit. The system was configured to measure GEM every 5 min., and ~~RGM~~GOM and PBM every 2 ~~two hr.~~h.

The details about the Tekran-based mercury speciation system can be found in Landis et al. (2002). In general, the automated measurement process can be summarized as sample collection, thermal desorption and determination. During the collection period, ambient air was drawn to the system at a flow rate of 10 L/min.

带格式的：字体颜色：自动设置

带格式的：字体颜色：自动设置

带格式的：字体颜色：自动设置

带格式的：字体颜色：自动设置

带格式的：字体颜色：自动设置

带格式的：中文(中国)

~~RGM~~GOM and PBM in the air were captured by a KCl-coated quartz annular denuder in the 1130 unit and a quartz filter in the 1135 unit, respectively, whereas GEM would pass through the denuder and filter and be quantified on the Tekran 2537B by cold-vapor atomic fluorescence spectroscopy (CVAFS). After an hour of sampling, the 1135 quartz filter and the 1130 denuder would be switched to the thermal decomposition mode at 800 ℃ and 500 ℃, respectively, with the resulting Hg^0 quantified by the 2537B unit in the next hour, while the 1135 and 1130 components were flushed with zero-mercury gas for the next sampling.

The instrument maintenance followed typical protocols used in similar studies ~~(Landis et al., 2002;Hu et al., 2014)~~(Landis et al., 2002;Hu et al., 2014). The quartz annular denuder was recoated every two weeks, the quartz filter was replaced once a month, and the Teflon filter (pore size 0.2 μm) in the sample inlet was changed every two weeks. Automated recalibration of the Tekran 2537B was performed every 25 h using an internal mercury permeation source. No calibration standards were available for ~~RGM~~GOM and PBM, but the 1σ precision for ~~RGM~~GOM and PBM was about 15 % ~~(Landis et al., 2002)~~(Landis et al., 2002). The detection limit in ambient air is about 0.5 ng m^{-3} for GEM (or TGM) at a resolution of 5 min, and 1 pg m^{-3} for ~~RGM~~GOM and PBM at a resolution of 2 h ~~(Gustin et al., 2015)~~(Gustin et al., 2015). Although the Tekran-based mercury speciation technique has been widely used around the world, recent studies have shown that the technique does not efficiently collect all gaseous oxidized mercury and thus may substantially underestimate the concentration of reactive mercury ~~(Huang et al., 2013;Gustin et al., 2013)~~(Huang et al., 2013;Gustin et al., 2013). Therefore, the ~~RGM~~GOM values reported in this study

带格式的：字体颜色：自动设置
带格式的：字体颜色：自动设置
带格式的：字体颜色：自动设置
带格式的：字体颜色：自动设置
带格式的：字体颜色：自动设置
带格式的：字体颜色：自动设置
带格式的：字体颜色：自动设置
带格式的：字体颜色：自动设置
带格式的：字体颜色：自动设置
带格式的：字体颜色：自动设置
带格式的：字体颜色：自动设置
带格式的：中文(中国)

should be considered as the lower ~~limits~~limit of gaseous oxidized mercury in the air ~~(Wang et al., 2014)~~(Wang et al., 2014).

2.3 Ancillary Data

Standard meteorological measurements including air temperature, air pressure, RH, wind direction and speed were observed with a 5-min resolution. CO was measured by an automated infrared carbon monoxide analyzer (Model EC9830T, Ecotech Inc., Australia), with a detction limit of 40 ppbv. O_3 was measured every 5 min by an ozone analyzer (Model EC9810B, Ecotech Inc., Australia); its detection limit and accuracy are 0.5 ppbv and 0.001 ppm, respectively. NO_2 was measured by a Multi axis differential optical absorption spectroscopy (MAX-DOAS) instrument. The collected spectra were analyzed using the QDOAS spectral fitting software suite developed at BIRA-IASB (http://uv-vis.aeronomie.be/software/QDOAS/). ~~We used the geometric approximation for conversion between slant column densities (SCDs) and vertical column densities (VCDs) (Ma et al., 2013). $PM_{2.5}$ (particulate matter less than 2.5 μm in diameter) data are collected from China air quality online analysis platform (http://www.aqistudy.cn/historydata/index.php). In addition, 24-hr PM_{10} (particulate matter less than 10 μm in diameter) samples were collected on glass fiber filters by a high volume sampler during heavy pollution episodes (from 10 Nov to 9 Dec 2013, n=11). Water-soluble ions in the PM_{10} samples were determined by ion chromatography (Model ICS-2100, Dionex). In order to identify the potential source of mercury, NASA's satellite hotspots/fire locations information were obtained from the Fire Information for Resource Management System (FIRMS) (https://firms.modaps.eosdis.nasa.gov/firemap/).~~$PM_{2.5}$ (particulate matter less than 2.5

带格式的：字体颜色：自动设置

带格式的：字体颜色：自动设置，英语(美国)

带格式的：字体颜色：自动设置

带格式的：行距：1.5 倍行距

带格式的：字体颜色：自动设置

带格式的：中文(中国)

μm in diameter) data are collected from China air quality online analysis platform (http://www.aqistudy.cn/historydata/index.php).

2.4 Potential Sources Contribution Function (PSCF) analysis

To identify the possible influence of long-range transport on the distribution of atmospheric mercury in Hefei, we calculated backward trajectories of air masses using the HYSPLIT (Hybrid Single-particle Lagrangian Integrated Trajectory) model with the Global Data Assimilation System (GDAS 1°) developed by the National Oceanic and Atmospheric Administration (NOAA) (*http://www.ready.noaa.gov*) (Draxler and Hess, 1998). Considering the atmospheric pollutants are mainly concentrated in the low altitude during heavy pollution days, the trajectory arrival heights were set at 500 m to represent the boundary layer where atmospheric pollutants were well mixed. ~~In this study, 5-day back-trajectories were calculated in ensemble forms which calculate 27 trajectories from the selected starting point (31°52′ N, 117°17′ E) (Fain et al., 2009).~~In this study, 3-day back-trajectories were generated hourly by TrajStat, a software including HYSPLIT for trajectory calculation (Wang et al., 2009).

The contributions of other pollution source regions to the atmospheric mercury at Hefei was identified by the Potential Sources Contribution Function (PSCF) analysis with the TrajStat software ~~(Wang et al., 2009).~~ PSCF analysis has been shown to be useful in spatially identifying pollution sources for pollutants with a long lifetime such as elemental mercury and CO ~~(Xu and Akhtar, 2010)~~(Xu and Akhtar, 2010). The PSCF values for the grid cells in the study domain were calculated by counting the trajectory segment endpoints that terminate within each cell. The number of endpoints

带格式的：字体颜色：自动设置

带格式的：行距：1.5 倍行距

带格式的：字体颜色：自动设置

带格式的：字体颜色：自动设置

带格式的：字体颜色：自动设置

带格式的：中文(中国)

that fall in the ij_{th} cell is designated as N_{ij}. The number of endpoints for the same cell corresponding to the atmospheric mercury concentration higher than an arbitrarily set criterion ~~(4 ng m^{-3} which was the~~is defined to be M_{ij}. In this study, mean GEM concentration of 4 ng m^{-3} during the whole study period~~) is defined to be M_{ij}~~, was used as the mercury pollution criterion. The PSCF value for the ij_{th} cell is then defined as:

~~$PSCF_{ij} = \frac{M_{ij}}{N_{ij}} W_{ij}$~~ $PSCF_{ij} = \frac{M_{ij}}{N_{ij}} W_{ij}$ (2)

W_{ij} is an arbitrary weight function to reduce the effect of small values of N_{ij}. The PSCF values were multiplied by W_{ij} to better reflect the uncertainty in the values for these cells ~~(Polissar et al., 2001)~~(Polissar et al., 2001). The weight function reduces the PSCF values when the total number of endpoints in a particular cell is less than 3 times the average value of the end points per cell:

~~$W_{ij} = \begin{cases} 1.0 & N_{ij} \geq 3N_{ave} \\ 0.70 & 3N_{ave} > N_{ij} \geq 1.5N_{ave} \\ 0.40 & 1.5N_{ave} > N_{ij} \geq N_{ave} \\ 0.20 & N_{ave} > N_{ij} \end{cases}$~~ $W_{ij} = \begin{cases} 1.0 & N_{ij} \geq 3N_{ave} \\ 0.70 & 3N_{ave} > N_{ij} \geq 1.5N_{ave} \\ 0.40 & 1.5N_{ave} > N_{ij} \geq N_{ave} \\ 0.20 & N_{ave} > N_{ij} \end{cases}$ (3)

3. Results

We intended to continuously monitor speciated atmospheric mercury concentration over the course of a year; however, interruptions were inevitable due to instrument maintenance, which resulted in loss of data for the following four periods: (1) 25 September to 9 October 2013; (2) 5-14 November 2013; (3) 9-25 February 2014; and (4) 1-14 April 2014. The rest of the data were grouped into haze days and

带格式的：字体颜色：红色

带格式的：字体颜色：红色

带格式的：字体颜色：红色

带格式的：字体颜色：自动设置

带格式的：字体颜色：自动设置

带格式的：字体颜色：自动设置

带格式的：中文(中国)

non-haze days according to the China Meteorological Administration's haze standard (QX/T 113-2010). Haze days refer to the days when the atmospheric visibility < 10 km and RH < 80% (Duan et al., 2016), and non-haze days refer to clear days with the atmospheric visibility > 10 km. The visibility and RH information were collected from the weather history data at the Luogang Airport of Hefei (http://www.wunderground.com/). Through the study period of almost a year, a total of 56 days were identified to be haze days, and 253 days to be non-haze days. All the times reported herein are local time (UTC + 8 ~~hr~~h).

3.1~~.~~ Overall characteristics of speciated atmospheric mercury

The time series of GEM, ~~RGM~~GOM and PBM concentrations at the study site throughout the study period are shown in Fig. 2, and their frequency distributions are shown in Fig. S1 (in the supporting information). The mean (± standard deviation) GEM, ~~RGM~~GOM and PBM concentrations during the whole study period were 4.07 ± 1.91 ng m^{-3}, 3.67 ± 5.11 pg m^{-3}, and 30.0 ± 100.3 pg m^{-3}, respectively (Table 1). The GEM concentrations in different seasons did not differ much. The highest GEM concentration occurred in autumn (4.51 ± 2.10 ng m^{-3}), while the lowest in spring (3.89 ± 1.79 ng m^{-3}). ~~RGM~~GOM concentrations varied greatly during the study period with much higher concentrations in autumn and the lowest in winter. A similar seasonal variation in the ~~RGM~~GOM concentration was observed at a remote site in Mt. Gongga of southwest China ~~(Fu et al., 2008b)~~(Fu et al., 2008b). The seasonal trend in PBM was also observed in Hefei with its concentration decreasing in the following order: autumn > winter > spring > summer. The mean PBM concentration during the cold season was about 20 times that in summer, similar to the findings

带格式的：字体颜色：自动设置
带格式的：字体颜色：自动设置
带格式的：字体颜色：自动设置
带格式的：字体颜色：自动设置
带格式的：字体颜色：自动设置
带格式的：字体颜色：自动设置
带格式的：字体颜色：自动设置，英语(美国)
带格式的：字体颜色：自动设置，英语(美国)
带格式的：字体颜色：自动设置
带格式的：字体颜色：自动设置
带格式的：字体颜色：自动设置
带格式的：字体颜色：自动设置
带格式的：字体颜色：自动设置
带格式的：中文(中国)

from many previous studies in China ~~(Zhang et al., 2013;Fu et al., 2011;Fu et al., 2008b;Fang et al., 2001)~~(Zhang et al., 2013;Fu et al., 2011;Fu et al., 2008b;Fang et al., 2001).

Comparisons of speciated atmospheric mercury concentrations with other urban and rural areas in China and a few other countries are shown in Table 2. The mean GEM concentration at Hefei is slightly higher than that in many remote areas in China ~~(Fu et al., 2008a;Fu et al., 2008b;Fu et al., 2012;Wan et al., 2009a;Wan et al., 2009b;Zhang et al., 2015a)~~(Fu et al., 2008a;Fu et al., 2008b;Fu et al., 2012;Wan et al., 2009a;Wan et al., 2009b;Zhang et al., 2015a), but is much lower than those in urban areas of industrial cities such as Guiyang and Changchun where large point sources of mercury exist (e.g., non-ferrous metal smelting, coal-fired power plants, and residential coal burning) ~~(Feng et al., 2004;Fu et al., 2011;Fang et al., 2004)~~(Feng et al., 2004;Fu et al., 2011;Fang et al., 2004). Although Hefei is geographically close to Shanghai, a mega urban centre in China, it is interesting to note that the TGM concentration of Shanghai is much lower than that of Hefei. This may be due to the fact that Shanghai is a coastal city that is influenced more by cleaner marine air masses ~~(Friedli et al., 2011)~~(Friedli et al., 2011). Table 2 also shows that the average concentration of GEM in Hefei is typically more than fold or two ~~folds~~ fold that in the urban and rural areas in Europe and North America ~~.~~ (Liu et al., 2010;Li et al., 2008;Brooks et al., 2010).

3.2 ~~.~~ Speciated atmospheric mercury during non-haze days

The frequency distribution of GEM, ~~RGM~~GOM and PBM for the non-haze period are shown in Fig. S1 (in blue). The mean concentration of GEM was 3.95 ± 1.93 ng

带格式的：字体颜色：自动设置
带格式的：字体颜色：自动设置
带格式的：字体颜色：自动设置
带格式的：字体颜色：自动设置
带格式的：行距：1.5 倍行距
带格式的：字体颜色：自动设置
带格式的：中文(中国)

m^{-3}. Its distribution was characterized by large fluctuations ranging from 0.2 to 23.8 ng m^{-3}, although more than half of the GEM values were in the narrow range 2-4 ng m^{-3}. The mean concentration of ~~RGM~~GOM was 2.49 ± 2.41 pg m^{-3} with a range of 0.5-33.5 pg m^{-3}, although most of the values were in the range of 1-4 pg m^{-3}. High concentrations of ~~RGM~~GOM (exceeding 10 pg m^{-3}) only accounted for 1.4% of the total data. The mean ~~RGM~~GOM concentration at the Hefei site is much smaller than that reported from other study sites in China (Table 2), but is comparable to the values observed from many European and North American sites ~~(Brooks et al., 2010;Li et al., 2008;Liu et al., 2010;Cheng et al., 2014)~~(Peterson et al., 2012;Cheng et al., 2014;Ren et al., 2016). The mean PBM concentraion at the Hefei site during the non-haze days was 23.3 ± 90.8 pg m^{-3} with an exceptionally large range of 0.5-1827 pg m^{-3}. The frequency distribution of PBM showed that high PBM concentrations (i.e., > 50 pg m^{-3}) accounted for 6.4% of the total data. The PBM concentration under the non-haze condition in Hefei is generally at a similar level to the remote areas, such as Mt. Gongga, Mt. Waliguan and Shangri-~~Li~~La in western China.

Diurnal variations of GEM, PBM and ~~RGM~~GOM concentrations for non-haze days are shown in Fig. 3. Both GEM and PBM concentrations exhibited similar variations with elevated concentrations during night. The ~~RGM~~GOM concentration during the daytime was slightly higher than that in nighttime, typically peaking between 10:00 and 12:00.

3.3~~.~~ Speciated atmospheric mercury during haze days

Haze pollution mainly occurred in December and January at our monitoring site. The four major haze pollution periods were identified in grey in Fig. 2. The mean

带格式的：字体颜色：自动设置
带格式的：字体颜色：自动设置
带格式的：字体颜色：自动设置
带格式的：字体颜色：自动设置
带格式的：字体颜色：自动设置
带格式的：字体颜色：自动设置
带格式的：缩进：首行缩进： 0.63 厘米，行距：1.5 倍行距
带格式的：字体颜色：自动设置
带格式的：行距：1.5 倍行距
带格式的：中文(中国)

concentrations of GEM, ~~RGM~~GOM and PBM during these haze days were 4.74 ± 1.62 ng m^{-3}, 4.32 ± 8.36 pg m^{-3} and 60.2 ± 131.4 pg m^{-3}, respectively (Table 1). The frequency distributions of GEM, ~~RGM~~GOM and PBM for the haze days are shown in Fig. S1 (in gray). Comparison of GEM, ~~RGM~~GOM and PBM concentrations during haze and non-haze days is shown in Fig. ~~4.~~S2. GEM, ~~RGM~~GOM and PBM concentrations show siginificant differences between haze and non haze days ($p<0.001$, t-test). On average, the concentration of GEM in haze days was 1.2 times that in non-haze days. Similarly, the concentration of ~~RGM~~GOM in haze days was about 1-1.7 times those in non-haze days. The largest impact of haze pollution is however on PBM, with the mean PBM concentration in haze days about 2.5 times that of non-haze days. High concentrations of ~~RGM~~GOM (exceeding 10 pg m^{-3}) and PBM concentrations (exceeding 50 pg m^{-3}) were also more frequently observed than in non-haze days, accounting for 5.9% and 25%, respectively, of the total haze days.

Diurnal variations of GEM, PBM and ~~RGM~~GOM concentrations for haze days are shown in Fig. 3. GEM concentrations were higher during night, decreased during daytime. The opposite pattern was observed for ~~RGM~~GOM, which showed higher concentrations during daytime than during night; the duration of the ~~RGM~~GOM peak also lasted longer for haze days. On the contrary, the PBM typically peaked just before sunrise, with the lowest values occurred in the afternoon (14:00-16:00).

4. Discussion

4.1 Influence of atmospheric mercury emission source

~~The statistically significant difference in the GEM concentration between non-haze days and haze days suggests that haze pollution could directly affect the concentration of elemental mercury.~~ In order to understand the mercury sources

带格式的：字体颜色：自动设置
带格式的：字体颜色：自动设置
带格式的：字体颜色：自动设置
带格式的：字体颜色：自动设置
带格式的：字体颜色：自动设置
带格式的：字体颜色：自动设置
带格式的：字体颜色：自动设置
带格式的：字体颜色：自动设置
带格式的：字体颜色：自动设置
带格式的：字体颜色：自动设置
带格式的：中文(中国)

attribution ~~during haze days~~, the PSCF model analysis was conducted by using the TrajStat software. ~~As shown in Fig. 5, the area south to the monitoring site and the neighboring provinces were the main sources region during haze days. Thus, atmospheric mercury in haze days were mainly affected by local or regional emission sources.~~

The seasonal sources could ~~also~~ be inferred from the PSCF analysis with the year-round data. Fig. ~~6(A)~~4a showed the overall spatial contribution of mercury emission sources in China. As Hefei is located in east-central China, its atmospheric mercury concentration could be affected by both north and south emission sources, including those from the North China Plain (especially Shandong Provice) and the neighboring provinces of Henan, Jiangsu, Jiangxi and Hubei. The total mercury emissions from Henan and Shandong provinces were estimated to be over 50 and 45 tons in 2010, respectively, making them two largest Hg emitters in China (Zhang et al., 2015b). Long-range transport could also impact the seasonal variations of atmospheric mercury in Hefei. As shown in Figure ~~6~~4, in spring, the major contributors of atmospheric mercury to Hefei were from the southwestern region including the local area and the Jiangxi and Hunan provinces. In summer, the main contributors were from north of Anhui, as well as Henan and Jiangxi provinces, and even from the Pearl River Delta region in the far south. ~~In autumn and winter, the prevalent seasons for haze pollution, the most important anthropogenic mercury sources to the monitoring site were the local emissions and those from the neighboring region of Shandong, Henan and the Yangtze River Delta region. The total mercury emissions from Henan and Shandong provinces were estimated to be over 50 and 45 tons in 2010, respectively, making them two largest Hg emitters in China (Zhang et al., 2015b).~~ Since the number of haze days accounts only for 5.6% of the total days in spring and summer, we did not provide haze and non-haze PSCF results

带格式的：字体颜色：自动设置

带格式的：字体颜色：自动设置

带格式的：行距：1.5 倍行距

带格式的：字体颜色：自动设置

带格式的：字体颜色：自动设置

带格式的：字体颜色：自动设置

带格式的：字体颜色：自动设置

带格式的：中文(中国)

for spring and summer seasons. As autumn and winter are the prevalent seasons for haze pollution, one PSCF result for haze days and another for non-haze days are shown for autumn and winter, respectively. The statistically significant difference ($p<0.001$) in the GEM concentration between non-haze days and haze days suggests that haze pollution could directly affect the concentration of elemental mercury. As shown in Figs. 4d and 4f, higher GEM concentration was mainly influenced by local emission sources during haze days. For non-haze days, the most important mercury sources to the monitoring site were not only the local emission sources, but also those from the neighboring region of Shandong, Henan and Jiangxi provinces (see Figs. 4e and 4g). In summary, the increase of GEM concentration during haze days was mainly caused by local emission.

~~GEM and CO normally share anthropogenic emission sources, such as industrial and domestic coal combustion (Wu et al., 2006). However, they also have their own sources, vehicles are another kind of dominant sources for CO, while power plants are another type of mainly sources for GEM. The correlation between the concentrations of GEM and CO during non-haze and haze days is shown in Fig. S2. The slope of the trend line represents the Hg/CO ratio. Emissions from power plants typically have a higher Hg/CO ratio (Wu et al., 2006), whereas biomass burning and residential coal combustion have a lower Hg/CO ratio due to incomplete combustion (Weiss-Penzias et al., 2007). The Hg/CO ratios from our study for both non-haze and haze days are in the range of 0.0003-0.0009 ng m^{-3} $ppbv^{-1}$, similar to the ratio reported for Alaska biomass burning (0.0014 ± 0.0006 ng m^{-3} $ppbv^{-1}$; Weiss-Penzias et al., 2007), indicating that biomass burning might have played an important role in mercury emission in Hefei. This is further supported by the concentration of water-soluble~~

带格式的：字体颜色：红色

带格式的：中文(中国)

~~potassium (K^+) in PM_{10}. K^+ is a typical component of biomass burning aerosol and has been used as a tracer element for qualitative identification of biomass burning (Cachier et al., 1991). As shown in Fig. S3, K^+ in PM_{10} shows a good correlation with air quality index (AQI) during the heavy pollution period of Nov-Dec, 2013. In addition, seven high GEM events were identified during the whole monitoring period (Table S1). 5-day backward trajectories for each GEM heavy pollution event for the time of at maximum GEM concentration are shown in Fig. S4. Air masses with elevated GEM concentration were mainly from NW, SW and East directions. In combination with the NASA's satellite hotspots/fire locations information from the Fire Information for Resource Management System (FIRMS), there were potential biomass burning occurred in these regions when air masses passed over (Fig. S4, Events 1-7). Therefore, biomass burning can contribute to the observed higher mercury concentrations, which not only came from local sources (Events 1 and 4), but could also be affect by other regions through long-range transport processes (Events 2, 3, 6 and 7).~~

GEM and CO often share anthropogenic emission sources, such as industrial coal combustion, domestic coal combustion, iron and steel production and cement production (Wu et al., 2006;Wang et al., 2005). However, they also have their own sources. For instance, power plants and nonferrous metal smelters emit mercury but hardly any CO, while most of CO originates from vehicles which are not a major emitter for mercury. The correlation coefficients and slopes between GEM concentration and CO concentration during pollution events are shown in Table 3. These mercury pollution episodes were defined as a period with hourly average GEM concentration higher than seasonal average GEM concentration and the duration of elevated hourly GEM concentration lasted for over 10 hours. The Hg/CO slope and

带格式的：中文(中国)

correlation between GEM and CO concentrations has been used to identify long-range transport episodes and local episodes in previous research (Jaffe et al., 2005;Weiss-Penzias et al., 2006;Kim et al., 2009). These episodes could classified into long-range transport episodes or local episode by using the correlation coefficients (R^2) of linear regression: significant positive correlation for long-range transport episodes and poor correlation for local episodes (Kim et al., 2009). Six episodes (events: 1-6) were found to have poor correlations between GEM and CO concentrations (R^2: 0.01-0.29) for local episodes, while four episodes (events: 7-10) were found to have positive correlations between GEM and CO concentrations (R^2: 0.51-0.79) for long-range transport episodes. These local episodes tend to occur in autumn and winter. The slope of the trend line represents the Hg/CO ratio. Emissions from power plants typically have a higher Hg/CO ratio (Wu et al., 2006), whereas residential coal and biomass burning combustion have a lower Hg/CO ratio (0.0013-0.0046 ng m^{-3} $ppbv^{-1}$) due to incomplete combustion (Weiss-Penzias et al., 2007). The Hg/CO ratio for vehicles is nearly zero (Zhang et al., 2013). The Hg/CO ratios from our study for pollution episodes are in the range of 0.0001-0.0050 ng m^{-3} $ppbv^{-1}$. In summary, the low GEM/CO ratio in Hefei might related to the local incomplete combustion, like residential coal and biomass burning combustion.

4.2 Impacts of meteorological factors for atmospheric mercury during haze days

Meteorological ~~condition~~conditions, especially wind direction and speed, could also impact the atmospheric mercury during haze days. The wind rose for the monitoring site during the study period is shown in Fig. ~~7~~5. Easterly and southeasterly winds represented the prevailing wind directions at the study site. A wind rose

带格式的：字体颜色：自动设置

带格式的：字体颜色：自动设置

带格式的：字体颜色：自动设置

带格式的：中文(中国)

diagram of GEM concentrations above the 90th percentile value is shown in Fig. ~~7B~~5B. We found that 67% of the high GEM concentrations occurred at low wind speed (below 1.5 m s^{-1}); however, wind speed below 1.5 m s^{-1} accounted for only 1.7% of total study. High ~~RGM~~GOM and PBM concentrations appear not to be related to high wind speed (wind speed: 3-5 m s^{-1}); only 1.4% and 2.6% of the high ~~RGM~~GOM and PBM concentrations were observed under high wind-speed conditions, respectively (Figs. ~~7C~~5C and ~~7D~~5D). In general, most of the high atmospheric mercury levels occurred in the low wind speed conditions. This slow wind speed condition is not conductive to the spread of mercury and thus favours the accumulation of atmospheric mercury, especially during haze days. This result is further support that atmospheric mercury during haze days is mainly affected by local emissions.

Both GEM and PBM concentrations exhibited great variations with elevated concentration during night or early morning, regardless of the presence of haze. Such a diurnal variation of GEM and PBM could be related to changes in the height of urban boundary layer, which is typically low in the morning and night, and high during the daytime ~~(Yuan et al., 2005~~(Yuan et al., 2005;Mao et al., 2006). The maximum PBM concentration (observed at 6:00) was more than 4 times higher than the minimum value (observed at 16:00) both under non-haze and haze days, and about 76% PBM were ~~removed~~declined during this period (6:00-16:00). However, the reductions of PBM as a result of deposition during haze days was 62.7 pg m^{-3}, which was about 2.4 times that in non-haze days, suggesting that haze pollution could increase the removal of PBM and thus reduce its atmospheric lifetime. Although PBM is not the major form of mercury emitted to the atmosphere, it is crucial in atmospheric mercury transport and removal

带格式的：字体颜色：自动设置

带格式的：字体颜色：自动设置

带格式的：字体颜色：自动设置

带格式的：字体颜色：自动设置

带格式的：字体颜色：自动设置

带格式的：字体颜色：自动设置

带格式的：行距：1.5 倍行距

带格式的：字体颜色：自动设置

带格式的：中文(中国)

processes due to its short atmospheric lifetime. As shown in Fig. 6, highest PBM and $PM_{2.5}$ concentrations were observed in January, which most likely due to shallower boundary layer in January than in other months. The co-variation in February is weaker, possibly due to the loss of PBM data because of instrument maintenance (see Section 2.3). ~~8, the~~The PBM concentration co-varied with the $PM_{2.5}$ concentration, especially in January when all the four PBM peak events were associated with increased $PM_{2.5}$ concentrations~~.~~ (Fig. 6c). This result indicates that the $PM_{2.5}$ concentration may play an important role in the formation of PBM. Thus, elevated~~The co-variation in February is weaker, possibly due to the loss of PBM data because of instrument maintenance (see Section 2.3). Elevated~~ PBM concentrations might be due to the poor diffusion conditions in cold months and high PM pollution. ~~Although the concentrations of $PM_{2.5}$ were similar from March to June, March showed higher PBM concentrations. This might be due to higher temperatures in the warmer months which do not favor mercury adsorption (Otani et al., 1986). These results indicate that both the $PM_{2.5}$ concentration and temperature may play an important role in the formation of PBM.~~

4.3 ~~Chemical process for RGM~~Enhancements in GOM and the potential oxidation mechanism

~~In contrast with the diurnal variations of GEM and PBM, RGM shows different diurnal trend. The RGM concentration during daytime was slightly higher than at night. As discussed before in 4.2 section, the diurnal variation of GEM and PBM could be related to changes in the height of urban boundary layer. So the role of boundary layer for the enhancement of RGM during daytime would be limited. The weak correlation ($r=0.164$, $p<0.001$) between RGM and CO suggests that regional anthropogenic sources are not a major source of RGM in the air. As shown in Fig. 9 (haze days), the peak value of RGM coincided well with the lowest value of CO, suggesting that the production of RGM in haze days does not fully come from~~

带格式的：字体颜色：自动设置

带格式的：字体颜色：自动设置

带格式的：字体颜色：自动设置

带格式的：字体颜色：红色

带格式的：字体颜色：自动设置

带格式的：字体颜色：自动设置

带格式的：字体颜色：红色

带格式的：缩进：首行缩进： 0 字符，行距：1.5 倍行距

带格式的：行距：1.5 倍行距

带格式的：字体颜色：红色

带格式的：中文(中国)

anthropogenic emission sources. Instead, RGM is more likely produced from the in situ oxidation of GEM; this is supported by the fact that the peak values of RGM coincided well with the decline of GEM. We found that the RGM concentration did not change much from 8:00 to 20:00 (local time) during haze days. This indicates that photochemical reaction between GEM and RGM still takes place during haze days, but the daytime change in the intensity of solar radiation has been greatly dampened due to the light-haze interaction.

Various atmospheric oxidants are capable of oxidizing GEM to RGM, including halogen radicals, ozone, hydroxyl radicals (OH), among others (Holmes et al., 2010;Wang et al., 2014). Halogen radicals, especially bromine atoms, are believed to be the the primary oxidant for GEM in the global tropopshere (Holmes et al., 2010). Unfortunately, we did not measure halogen radicals in this study. Ozone itself is not an efficient oxidant for GEM oxidation due to low reaction rate (Hall, 1995;Holmes et al., 2010). In the lower troposphere, ozone is produced from daytime photochemical reactions involving volatile organic compounds (VOC) and nitrogen oxides (NO_x). Due to fresh emissions of NO from vehicles can react with O_3 to form NO_2, so ozone could not fully represent photochemical oxidation processes in urban area (Herndon et al., 2008). Compared with ozone, odd oxygen (O_X = O_3+NO_2) is a more conserved tracer of the extent of photochemical processing in the urban atmosphere (Herndon et al., 2008;Wood et al., 2010). Because of such NO_2 concentrations from MAX-DOAS are available only during the daytime, so we could only use O_X to be a indicator for GEM oxidation occurred in the daytime. Diurnal variations of GEM, RGM and Gas-Phase Data (O_X, O_3, NO_2 and CO) concentrations during non-haze and haze days are shown in Fig. 9. The increase of O_X is consistent with the increase of RGM during haze days, but seems to lag behind the increase of RGM during non-haze days, suggesting some oxidation processes might be at work during haze days. During haze days, both the RGM and O_X reached highest values around 16:00, along with the lowest value of GEM, indicating the chemical transformation between GEM and RGM occurred. However, this phenemenon is not found in non-haze days.

The OH radical is also an important oxidant for mercury in the atmosphere. Previous studies have shown that the major source of OH in the early morning is the photolysis of HONO, which accumulates in the urban atmospheric boundary layer during night (Kleffmann et al., 2005). The formation of HgOH as an intermediate product of the Hg^0(g) + OH oxidation reactions has been proposed by (Sommar et al., 2001), although HgOH is highly unstable and could decompose back rapidly to Hg^0 and OH (Goodsite et al., 2004). It has been proposed that secondary reactants such as

带格式的：中文(中国)

~~NO_2, HO_2, RO, RO_2, and NO could assist the formation of Hg(II) from the initial HgOH intermediate, which outcompetes with the decomposition of HgOH (Calvert and Lindberg, 2005). As an example, we calculated the transformation between GEM and RGM under the influence of NO_2, using the reactions and rate constants shown in Table S2. As shown in Fig. S5, the production rate of NO_2HgOH, $d[NO_2HgOH]/dt$, increased almost linearly with increasing NO_2 under low NO_2 concentrations, and eventually reached a steady state when the NO_2 concentration is high enough.~~

Diurnal variations of GEM, GOM, O_3 and CO concentrations during non-haze and haze days are shown in Fig. 7. The weak correlation ($r=0.164$, $p<0.001$) between GOM and CO suggests that the CO-producing, primary emission is not a major source of GOM in the air. This is clearly shown in Fig. 7 (haze days), where the peak value of GOM coincided with the lowest value of CO. GOM also shows a diurnal trend that is opposite to that of GEM and PBM; for both non-haze and haze days, GOM concentrations remained relatively constant during night, but increased rapidly prior to sunrise. Two processes can affect the GOM concentrations in the boundary layer air. The first is due to transport of GOM from the free troposphere (FT). It is well established that FT contains higher GOM concentrations than in the boundary layer(e.g., (Murphy et al., 2006;Lyman and Jaffe, 2012;Timonen et al., 2013;Brooks et al., 2014;Shah et al., 2016)). It is thus possible that higher GOM concentrations observed prior to sunrise is due to admixing from the free troposphere as the height of the boundary layer increases during the morning. In addition, in situ photochemical oxidation of GEM could also increase the concentration of GOM during daytime. Various atmospheric oxidants are capable of oxidizing GEM to GOM, including halogen radicals, ozone, hydroxyl radicals (OH), among others (Holmes et al., 2010;Wang et al., 2014).

To determine the relative importance of FT transport and in situ photochemical oxidation, we examined the relationship between GOM and the changes in the height

带格式的：中文(中国)

of the atmospheric boundary layer and the odd oxygen ($O_X = O_3+NO_2$) concentrations. We used O_x because it is a more conserved tracer of the extent of photochemical processes in the urban atmosphere (Herndon et al., 2008;Wood et al., 2010), as O_3 reacts with NO emitted from automobiles to form NO_2. Example results are shown in Fig. 8 for 20th November, 2013. As can be seen from the figure, both GOM and O_X reached higher concentrations from 12:00 to 16:00, along with the lowest value of GEM. The height of the atmospheric boundary layer changed very little (less than 0.1 km) over the same period (see Fig. S3). This simple comparison suggests that the transport of FT GOM might be limited and that at least some of the GOM were formed from in situ oxidation of GEM. Note that in our studies we could only calculate daytime O_x concentrations, because NO_2 concentrations from MAX-DOAS were only available during daytime.

We further investiagted the mechanism of the GEM oxidation to GOM. Ozone itself is not an efficient oxidant for GEM oxidation due to the low reaction rate (Hall, 1995;Holmes et al., 2010). Instead, halogen radicals (especially bromine atoms) and halogen radicals, are believed to be the primary oxidants for GEM in the global troposphere (Holmes et al., 2010). Unfortunately, we did not measure halogen radicals in this study. OH radicals are known to be present in the early morning urban boundary layer, primarily from the photolysis of HONO, which accumulates during night (Kleffmann et al., 2005). Therefore, here we consider the oxdiation of GEM by OH radicals. The formation of HgOH as an intermediate product of the Hg^0 (g) + OH oxidation reactions has been proposed by Sommar et al., 2001, although HgOH is highly unstable and could decompose back rapidly to Hg^0 and OH (Sommar et al., 2001;Goodsite et al., 2004). It has been proposed that the presence of other gases X

带格式的：中文(中国)

(X = NO_2, HO_2, RO, RO_2, or NO) could assist the formation of Hg(II) by forming X-HgOH, which outcompetes the decomposition of HgOH (Calvert and Lindberg, 2005;Dibble et al., 2012;Wang et al., 2014). As an example, we calculated the transformation between GEM and GOM under the influence of NO_2, using the reactions and rate constants shown in Table S1. As shown in Fig. S4, the production rate of NO_2HgOH, d[NO_2HgOH]/dt, increased almost linearly with increasing NO_2 under low NO_2 concentrations, and eventually reached a steady state when the NO_2 concentration is high enough.

Based on the production rate of NO_2HgOH, we can estimate the production of NO_2HgOH during the 1 hr sampling period when ~~RGM~~GOM was captured by the KCl-coated denuder in the Tekran 1130 unit. ~~As discussed earlier, a distinct diurnal relationship between GEM and RGM was observed both in non-haze and haze days (Fig. 9).~~ The production of NO_2HgOH and d[NO_2HgOH]/dt corresponding to different NO_2 concentrations is shown in Table ~~3.~~4. With the increase of the NO_2 concentration, the contribution of the NO_2HgOH production to ~~RGM~~GOM will increase. If the NO_2 concentration is within 100 ppbv (from 0 to 100 ppbv), the production of NO_2HgOH would be in range of 0.058-4.81 pg m^{-3} during the 1h sampling period. ~~The mean NO_2 concentration during haze days is 24.3 ppbv (unit convertion see the supporting information), which is higher that in non-haze days (17.4 ppbv). The increments of RGM from sunrise to peak (6:00-12:00) are about 2.14 pg m^{-3} (growth rate ≈ 0.36 pg m^{-3} h^{-1}) and 0.41 pg m^{-3} (growth rate ≈ 0.068 pg m^{-3} h^{-1}) during haze days and non-haze days, respectively.~~ As illustrated in Table ~~3~~4, the level of NO_2 observed in ~~the urban atmosphere~~our study is high enough ~~for~~to make increase the GOM production ~~of RGM during the 1h sampling period. In~~

带格式的：字体颜色：自动设置
带格式的：行距：1.5 倍行距
带格式的：字体颜色：自动设置
带格式的：字体颜色：自动设置
带格式的：字体颜色：自动设置
带格式的：字体颜色：自动设置
带格式的：字体颜色：自动设置
带格式的：字体颜色：自动设置
带格式的：字体颜色：自动设置
带格式的：字体颜色：自动设置
带格式的：字体颜色：自动设置
带格式的：字体颜色：自动设置
带格式的：字体颜色：自动设置
带格式的：字体颜色：自动设置
带格式的：中文(中国)

~~addition, we found that the NO_2 concentrations increased rapidly after sunrise to reach peak values around noon, consistent with the increases of RGM during haze days. We~~. Our results thus ~~postulates~~support a recent study in the tropical equatorial Pacific (Wang et al., 2014) that NO_2 aggregation with HgOH ~~may be~~provides provides a possible mechanism to explain the enhanced production of ~~RGM during the daytime over the inland urban air. The NO_2 level in urban air~~ GOM and the role of NO_2 might ~~have a~~ be more important ~~influence on the chemical transformations between the GEM and RGM during haze days, rather than non-haze days. But unfortunately, we can not provide an adequate description about these oxidation processes. To solve this problem, new~~in the urban air. More laboratory and ~~mercury model~~modeling studies on mercury oxidation mechanism ~~are needed~~in the presence of NO_2 and other gases are thus warranted.

5. Summary

Continuous measurements of speciated atmospheric mercury were conducted at Hefei, a mid-latitude inland city in central China, from July 2013 to June 2014. Measurements of other trace gases (e.g. CO, O_3, NO_2) and meteorological parameters were employed to better understand the sources and oxidation pathways of atmospheric mercury. The mean GEM, ~~RGM~~GOM and PBM concentrations during haze days were 4.74 ±1.62 ng m^{-3}, 4.32 ± 8.36 pg m^{-3} and 60.2 ± 131.4 pg m^{-3}, respectively. Potential source contribution function (PSCF) analysis suggested that the local mercury emission rather than long-range transport is the most important contributor of atmospheric mercury pollution during haze days at our monitoring site. ~~The Hg/CO ratio and NASA's satellite fire locations information indicated that the~~

带格式的：字体颜色：红色
带格式的：字体颜色：红色
带格式的：字体颜色：红色
带格式的：字体颜色：红色
带格式的：字体颜色：红色
带格式的：字体颜色：自动设置
带格式的：字体颜色：自动设置
带格式的：字体颜色：自动设置
带格式的：字体颜色：自动设置
带格式的：字体颜色：自动设置
带格式的：中文(中国)

~~biomass burning may plays an important role in mercury emission. Haze pollution has considerable impact on PBM rather than on GEM and RGM. Both GEM and PBM concentrations exhibited greatly variations with elevated concentration during night. The diurnal variations of GEM and PBM might be related to the boundary layer depth; a lower boundary layer depth in the morning and night could elevate the mercury concentration. The slow wind speed condition is not conductive to the spread of mercury and thus favours the accumulation of atmospheric mercury, especially during haze days. We found that PBM concentrations co-varied with the $PM_{2.5}$ concentration especially in January when all the four PBM peak events were associated with increased $PM_{2.5}$ concentrations. In addition,~~The low GEM/CO ratio in Hefei could be a result of local incomplete combustion sources such as residential coal and biomass burning. Haze pollution has a more profund impact on PBM than on GEM and GOM. PBM showed a remarkable seasonal pattern, with higher concentrations in cold seasons and lower in warm seasons. Elevated PBM concentrations might be due to both the high loadings of particle matter and disadvantageous diffusion conditions during haze days especially in cold months. ~~The peaks of RGM were observed around noon, which is probably due to the higher intensity of solar radiation~~Both GEM and ~~photochemical oxidation processes at this time. Change in the odd oxygen (O_X = O_3+NO_2)~~PBM concentrations exhibited great variations with elevated concentration ~~is normally appllied to be an indicator for photochemical reaction. The increase of O_X is consistent with the increase of RGM~~ during ~~haze days, but seems to lag behind the increase of RGM during non-haze days, suggesting some oxidation processes~~night. The diurnal variations of GEM and PBM might be ~~at work~~related to the boundary

带格式的：字体颜色：自动设置

带格式的：字体颜色：自动设置

带格式的：字体颜色：自动设置

带格式的：字体颜色：自动设置，英语(美国)

带格式的：字体颜色：自动设置

带格式的：中文(中国)

layer depth; a lower boundary layer depth in the morning and night could elevate the mercury concentration.

Unlike with the diurnal variations of GEM and PBM, GOM concentration remained relatively constant during night, and then increased rapidly prior to the sunrise. The enhancement of GOM during ~~haze days.~~daytime could be due to both the transport of GOM-enriched free troposphere air to the boundary layer and in situ oxidation of GEM in the boundary layer. Simple photochemical modeling supports the occurrence of daytime oxidation of GEM to GOM. Based on HgOH as an intermediate product, ~~we~~our calculations suggest that NO_2 aggregation with HgOH is a potential mechanism to explain the enhanced production of ~~RGM during the daytime over the inland urban air. The NO_2 level in urban air might have a more important influence on the chemical transformations between the GEM and RGM during haze days, rather than non-haze days~~GOM over the inland urban air.

Acknowledgements

This research was supported by grants from the National Basic Research Program of China (2013CB430000), the National Natural Science Foundation of China (Project Nos. 91544103,41575021) and the External Cooperation Program of BIC, CAS (Project No.211134KYSB20130012).

带格式的：缩进：首行缩进： 0.85 厘米，行距：1.5 倍行距，制表位：不在 32.91 字符

带格式的：字体颜色：红色

带格式的：字体颜色：红色

带格式的：字体颜色：红色

带格式的：字体颜色：红色

带格式的：行距：1.5 倍行距

带格式的：字体颜色：自动设置

带格式的：字体颜色：自动设置

带格式的：正文，行距：1.5 倍行距

带格式的：中文(中国)

References

Brooks, S., Luke, W., Cohen, M., Kelly, P., Lefer, B., and Rappenglück, B.: Mercury species measured atop the Moody Tower TRAMP site, Houston, Texas, Atmospheric Environment, 44, 4045-4055, 2010.

~~Cachier, H., Ducret, J., Bremond, M., Yoboue, V., Lacaux, J., Gaudichet, A., and Baudet, J.: Biomass burning aerosols in a savanna region of the Ivory Coast, in: Global biomass burning. Atmospheric, climatic, and biospheric implications, 1991.~~

Brooks, S., Ren, X., Cohen, M., Luke, W. T., Kelley, P., Artz, R., Hynes, A., Landing, W., and Martos, B.: Airborne vertical profiling of mercury speciation near Tullahoma, TN, USA, Atmosphere, 5, 557-574, 2014.

Calvert, J. G., and Lindberg, S. E.: Mechanisms of mercury removal by O_3 and OH in the atmosphere, Atmospheric Environment, 39, 3355-3367, 2005.

Chen, L.-W. A., Chow, J. C., Doddridge, B. G., Dickerson, R. R., Ryan, W. F., and Mueller, P. K.: Analysis of a summertime $PM_{2.5}$ and haze episode in the mid-Atlantic region, Journal of the Air & Waste Management Association, 53, 946-956, 2003.

Cheng, I., Zhang, L., Mao, H., Blanchard, P., Tordon, R., and Dalziel, J.: Seasonal and diurnal patterns of speciated atmospheric mercury at a coastal-rural and a coastal-urban site, Atmospheric Environment, 82, 193-205, ~~doi:10.1016/j.atmosenv.2013.10.016, 2014.~~2014.

~~Dommergue, A., Ferrari, C. P., Planchon, F. A., and Boutron, C. F.: Influence of anthropogenic sources on total gaseous mercury variability in Grenoble suburban air (France), Science of the total environment, 297, 203-213, 2002.~~

Dibble, T., Zelie, M., and Mao, H.: Thermodynamics of reactions of ClHg and BrHg radicals with atmospherically abundant free radicals, Atmospheric Chemistry and Physics, 12, 10271-10279, 2012.

带格式的：行距：1.5 倍行距

带格式的：中文(中国)

Draxler, R. R., and Hess, G.: An overview of the HYSPLIT_4 modelling system for trajectories, Australian meteorological magazine, 47, 295-308, 1998.

Duan, L., Xiu, G., Feng, L., Cheng, N., and Wang, C.: The mercury species and their association with carbonaceous compositions, bromine and iodine in $PM_{2.5}$ in Shanghai, Chemosphere, 146, 263-271, 2016.

~~Fain, X., Obrist, D., Hallar, A., Mccubbin, I., and Rahn, T.: High levels of reactive gaseous mercury observed at a high elevation research laboratory in the Rocky Mountains, Atmospheric Chemistry and Physics, 9, 8049-8060, 2009.~~

Fang, F., Wang, Q., and Li, J.: Atmospheric particulate mercury concentration and its dry deposition flux in Changchun City, China, Science of the total environment, 281, 229-236, 2001.

Fang, F., Wang, Q., and Li, J.: Urban environmental mercury in Changchun, a metropolitan city in Northeastern China: source, cycle, and fate, Science of the Total Environment, 330, 159-170, 2004.

Fang, G.-C., Wu, Y.-S., and Chang, T.-H.: Comparison of atmospheric mercury (Hg) among Korea, Japan, China and Taiwan during 2000–2008, Journal of hazardous materials, 162, 607-615, 2009.

Feng, X., Shang, L., Wang, S., Tang, S., and Zheng, W.: Temporal variation of total gaseous mercury in the air of Guiyang, China, Journal of Geophysical Research: Atmospheres (1984–2012), 109, 2004.

Friedli, H., Arellano Jr, A., Geng, F., Cai, C., and Pan, L.: Measurements of atmospheric mercury in Shanghai during September 2009, Atmospheric Chemistry and Physics, 11, 3781-3788, 2011.

带格式的：行距：1.5 倍行距

带格式的：行距：1.5 倍行距

带格式的：中文(中国)

Fu, X., Feng, X., Zhu, W., Wang, S., and Lu, J.: Total gaseous mercury concentrations in ambient air in the eastern slope of Mt. Gongga, South-Eastern fringe of the Tibetan plateau, China, Atmospheric Environment, 42, 970-979, 2008a.

Fu, X., Feng, X., Zhu, W., Zheng, W., Wang, S., and Lu, J. Y.: Total particulate and reactive gaseous mercury in ambient air on the eastern slope of the Mt. Gongga area, China, Applied Geochemistry, 23, 408-418, 2008b.

Fu, X., Feng, X., Qiu, G., Shang, L., and Zhang, H.: Speciated atmospheric mercury and its potential source in Guiyang, China, Atmospheric Environment, 45, 4205-4212, 2011.

Fu, X., Feng, X., Liang, P., Zhang, H., Ji, J., and Liu, P.: Temporal trend and sources of speciated atmospheric mercury at Waliguan GAW station, Northwestern China, Atmospheric Chemistry and Physics, 12, 1951-1964, 2012.

Goodsite, M. E., Plane, J., and Skov, H.: A theoretical study of the oxidation of Hg^0 to $HgBr_2$ in the troposphere, Environmental science & technology, 38, 1772-1776, 2004.

Gustin, M., and Jaffe, D.: Reducing the uncertainty in measurement and understanding of mercury in the atmosphere, Environmental science & technology, 44, 2222-2227, 2010.

Gustin, M., Amos, H., Huang, J., Miller, M., and Heidecorn, K.: Measuring and modeling mercury in the atmosphere: a critical review, Atmospheric Chemistry and Physics, 15, 5697-5713, 2015.

Gustin, M. S., Huang, J., Miller, M. B., Peterson, C., Jaffe, D. A., Ambrose, J., Finley, B. D., Lyman, S. N., Call, K., and Talbot, R.: Do we understand what the mercury

带格式的：中文(中国)

speciation instruments are actually measuring? Results of RAMIX, Environmental science & technology, 47, 7295-7306, 2013.

Hall, B.: The gas phase oxidation of elemental mercury by ozone, in: Mercury as a Global Pollutant, Springer, 301-315, 1995.

Herndon, S. C., Onasch, T. B., Wood, E. C., Kroll, J. H., Canagaratna, M. R., Jayne, J. T., Zavala, M. A., Knighton, W. B., Mazzoleni, C., and Dubey, M. K.: Correlation of secondary organic aerosol with odd oxygen in Mexico City, Geophysical Research Letters, 35, 2008.

Holmes, C. D., Jacob, D. J., Corbitt, E. S., Mao, J., Yang, X., Talbot, R., and Slemr, F.: Global atmospheric model for mercury including oxidation by bromine atoms, Atmospheric Chemistry and Physics, 10, 12037-12057, 2010.

Hu, Q.-. H., Kang, H., Li, Z., ~~Wangv~~Wang, Y.-. S., Ye, P.-. P., Zhang, L.-. L., Yu, J., Yu, X.-. W., Sun, C., and Xie, Z.-. Q.: Characterization of atmospheric mercury at a suburban site of central China from wintertime to springtime, Atmospheric Pollution Research, 5, 769-778, 2014.

Huang, J., Miller, M. B., Weiss-Penzias, P., and Gustin, M. S.: Comparison of gaseous oxidized Hg measured by KCl-coated denuders, and nylon and cation exchange membranes, Environmental science & technology, 47, 7307-7316, 2013.

Jaffe, D., Prestbo, E., Swartzendruber, P., Weiss-Penzias, P., Kato, S., Takami, A., Hatakeyama, S., and Kajii, Y.: Export of atmospheric mercury from Asia, Atmospheric Environment, 39, 3029-3038, 2005.

Kim, S.-H., Han, Y.-J., Holsen, T. M., and Yi, S.-M.: Characteristics of atmospheric speciated mercury concentrations (TGM, Hg (II) and Hg (p)) in Seoul, Korea, Atmospheric Environment, 43, 3267-3274, 2009.

带格式的：中文(中国)

Kleffmann, J., Gavriloaiei, T., Hofzumahaus, A., Holland, F., Koppmann, R., Rupp, L., Schlosser, E., Siese, M., and Wahner, A.: Daytime formation of nitrous acid: A major source of OH radicals in a forest, Geophysical Research Letters, 32, 2005.

Landis, M. S., Stevens, R. K., Schaedlich, F., and Prestbo, E. M.: Development and characterization of an annular denuder methodology for the measurement of divalent inorganic reactive gaseous mercury in ambient air, Environmental science & technology, 36, 3000-3009, 2002.

Li, J., Sommar, J., Wängberg, I., Lindqvist, O., and Wei, S.-q.: Short-time variation of mercury speciation in the urban of Göteborg during GÖTE-2005, Atmospheric Environment, 42, 8382-8388, 2008.

Lindberg, S., Bullock, R., Ebinghaus, R., Engstrom, D., Feng, X., Fitzgerald, W., Pirrone, N., Prestbo, E., and Seigneur, C.: A synthesis of progress and uncertainties in attributing the sources of mercury in deposition, AMBIO: A Journal of the Human Environment, 36, 19-33, 2007.

~~Lindberg, S. a., and Stratton, W.: Atmospheric mercury speciation: concentrations and behavior of reactive gaseous mercury in ambient air, Environmental Science & Technology, 32, 49-57, 1998.~~

Lindqvist, O., and Rodhe, H.: Atmospheric mercury-a review*, Tellus B, 37, 1985.

Liu, B., Keeler, G. J., Dvonch, J. T., Barres, J. A., Lynam, M. M., Marsik, F. J., and Morgan, J. T.: Urban–rural differences in atmospheric mercury speciation, Atmospheric Environment, 44, 2013-2023, 2010.

~~Ma, J., Beirle, S., Jin, J., Shaiganfar, R., Yan, P., and Wagner, T.: Tropospheric NO_2 vertical column densities over Beijing: results of the first three years of ground-based MAX-DOAS measurements (2008–2011) and satellite validation, Atmospheric Chemistry and Physics, 13, 1547-1567, 2013.~~

Lyman, S. N., and Jaffe, D. A.: Formation and fate of oxidized mercury in the upper troposphere and lower stratosphere, Nature Geoscience, 5, 114-117, 2012.

带格式的：行距：1.5 倍行距

带格式的：行距：1.5 倍行距

带格式的：中文(中国)

Mao, M., Jiang, W., Wu, X., Qi, F., Yuan, R., Fang, H., Liu, D., and Zhou, J.: LIDAR exploring of the UBL in downtown of the Nanjing City, Acta Scientiae Circumstantiae, 26, 1723-1728, 2006.

~~Otani, Y., Kanaoka, C., Usui, C., Matsui, S~~Marumoto, K., Hayashi, M., and ~~Emi, H.: Adsorption of~~ Takami, A.: Atmospheric mercury ~~vapor on particles~~concentrations at two sites in the Kyushu Islands, Japan, and evidence of long-range transport from East Asia, Atmospheric Environment, 117, 147-155, 2015.

Murphy, D., Hudson, P., Thomson, D., Sheridan, P., and Wilson, J.: Observations of mercury-containing aerosols, Environmental science & technology, ~~20, 735-738, 1986~~40, 3163-3167, 2006.

Pacyna, E. G., Pacyna, J. M., Steenhuisen, F., and Wilson, S.: Global anthropogenic mercury emission inventory for 2000, Atmospheric environment, 40, 4048-4063, 2006.

Pacyna, E. G., Pacyna, J., Sundseth, K., Munthe, J., Kindbom, K., Wilson, S., Steenhuisen, F., and Maxson, P.: Global emission of mercury to the atmosphere from anthropogenic sources in 2005 and projections to 2020, Atmospheric Environment, 44, 2487-2499, 2010.

Peterson, C., Alishahi, M., and Gustin, M. S.: Testing the use of passive sampling systems for understanding air mercury concentrations and dry deposition across Florida, USA, Science of the Total Environment, 424, 297-307, 2012.

Polissar, A. V., Hopke, P. K., and Harris, J. M.: Source regions for atmospheric aerosol measured at Barrow, Alaska, Environmental science & technology, 35, 4214-4226, 2001.

带格式的：行距：1.5 倍行距

带格式的：行距：1.5 倍行距

带格式的：行距：1.5 倍行距

带格式的：中文(中国)

Ren, X., Luke, W. T., Kelley, P., Cohen, M. D., Artz, R., Olson, M. L., Schmeltz, D., Goldberg, D. L., Ring, A., and Mazzuca, G. M.: Atmospheric mercury measurements at a suburban site in the Mid-Atlantic United States: Inter-annual, seasonal and diurnal variations and source-receptor relationships, Atmospheric Environment, 2016.

Schroeder, W. H., and Munthe, J.: Atmospheric mercury-an overview, Atmospheric Environment, 32, 809-822, 1998.

Shah, V., Jaeglé, L., Gratz, L., Ambrose, J., Jaffe, D., Selin, N., Song, S., Campos, T., Flocke, F., and Reeves, M.: Origin of oxidized mercury in the summertime free troposphere over the southeastern US, Atmospheric Chemistry and Physics, 16, 1511-1530, 2016.

Sommar, J., Gårdfeldt, K., Strömberg, D., and Feng, X.: A kinetic study of the gas-phase reaction between the hydroxyl radical and atomic mercury, Atmospheric Environment, 35, 3049-3054, 2001.

~~Stamenkovic, J., Lyman, S., and Gustin, M. S.: Seasonal and diel variation of atmospheric mercury concentrations in the Reno (Nevada, USA) airshed, Atmospheric Environment, 41, 6662-6672, 2007.~~

Streets, D. G., Hao, J., Wu, Y., Jiang, J., Chan, M., Tian, H., and Feng, X.: Anthropogenic mercury emissions in China, Atmospheric Environment, 39, 7789-7806, 2005.

Sun, Z., Mu, Y., Liu, Y., and Shao, L.: A comparison study on airborne particles during haze days and non-haze days in Beijing, Science of the total environment, 456, 1-8, 2013.

Timonen, H., Ambrose, J., and Jaffe, D.: Oxidation of elemental Hg in anthropogenic and marine airmasses, Atmospheric Chemistry and Physics, 13, 2827-2836, 2013.

带格式的：行距：1.5 倍行距

带格式的：行距：1.5 倍行距

带格式的：行距：1.5 倍行距

带格式的：中文(中国)

Wan, Q., Feng, X., Lu, J., Zheng, W., Song, X., Han, S., and Xu, H.: Atmospheric mercury in Changbai Mountain area, northeastern China I. The seasonal distribution pattern of total gaseous mercury and its potential sources, Environmental research, 109, 201-206, 2009a.

Wan, Q., Feng, X., Lu, J., Zheng, W., Song, X., Li, P., Han, S., and Xu, H.: Atmospheric mercury in Changbai Mountain area, northeastern China II. The distribution of reactive gaseous mercury and particulate mercury and mercury deposition fluxes, Environmental research, 109, 721-727, 2009b.

Wang, F., Saiz-Lopez, A., Mahajan, A., Mart ń, J. G., Armstrong, D., Lemes, M., Hay, T., and Prados-Roman, C.: Enhanced production of oxidised mercury over the tropical Pacific Ocean: a key missing oxidation pathway, Atmospheric Chemistry and Physics, 14, 1323, 2014.

Wang, L., Zhang, Q., Hao, J., and He, K.: Anthropogenic CO emission inventory of Mainland China, Acta Scientiae Circumstantiae, 25, 1580-1585, 2005.

Wang, Y., Zhang, X., and Draxler, R. R.: TrajStat: GIS-based software that uses various trajectory statistical analysis methods to identify potential sources from long-term air pollution measurement data, Environmental Modelling & Software, 24, 938-939, 2009.

Weigelt, A., Temme, C., Bieber, E., Schwerin, A., Schuetze, M., Ebinghaus, R., and Kock, H. H.: Measurements of atmospheric mercury species at a German rural background site from 2009 to 2011-methods and results, Environmental Chemistry, 10, 102-110, 2013.

Weiss-Penzias, P., Jaffe, D. A., Swartzendruber, P., Dennison, J. B., Chand, D., Hafner, W., and Prestbo, E.: Observations of Asian air pollution in the free troposphere at

带格式的：行距：1.5 倍行距

带格式的：行距：1.5 倍行距

带格式的：中文(中国)

Mount Bachelor Observatory during the spring of 2004, Journal of Geophysical Research: Atmospheres, 111, 2006.

Weiss-Penzias, P., Jaffe, D., Swartzendruber, P., Hafner, W., Chand, D., and Prestbo, E.: Quantifying Asian and biomass burning sources of mercury using the Hg/CO ratio in pollution plumes observed at the Mount Bachelor Observatory, Atmospheric Environment, 41, 4366-4379, 2007.

Wood, E., Canagaratna, M., Herndon, S., Onasch, T., Kolb, C., Worsnop, D., Kroll, J., Knighton, W., Seila, R., and Zavala, M.: Investigation of the correlation between odd oxygen and secondary organic aerosol in Mexico City and Houston, Atmospheric Chemistry and Physics, 10, 8947-8968, 2010.

Wu, Y., Wang, S., Streets, D. G., Hao, J., Chan, M., and Jiang, J.: Trends in anthropogenic mercury emissions in China from 1995 to 2003, Environmental science & technology, 40, 5312-5318, 2006.

Xu, X., and Akhtar, U.: Identification of potential regional sources of atmospheric total gaseous mercury in Windsor, Ontario, Canada using hybrid receptor modeling, Atmospheric Chemistry and Physics, 10, 7073-7083, 2010.

Yuan, S., Xin, Y., and Zhou, J.: Lidar Observations of the Lower Atmosphere in Hefei, Chinese Journal of Atmospheric Sciences, 29, 387-395, 2005.

Zhang, H., Fu, X., Lin, C., Wang, X., and Feng, X.: Observation and analysis of speciated atmospheric mercury in Shangri-La, Tibetan Plateau, China, Atmospheric Chemistry and Physics, 15, 653-665, 2015a.

Zhang, L., Wang, S., Wang, L., and Hao, J.: Atmospheric mercury concentration and chemical speciation at a rural site in Beijing, China: implications of mercury emission sources, Atmospheric Chemistry and Physics, 13, 10505-10516, 2013.

带格式的：行距：1.5 倍行距

带格式的：中文(中国)

Zhang, L., Wang, S., Wang, L., Wu, Y., Duan, L., Wu, Q., Wang, F., Yang, M., Yang, H., and Hao, J.: Updated Emission Inventories for Speciated Atmospheric Mercury from Anthropogenic Sources in China, Environmental science & technology, 49, 3185-3194, 2015b.

带格式的：中文(中国)

Table 1. Summary of GEM, ~~RGM~~GOM and PBM concentrations measured in Hefei from July 2013 to June 2014.

	GEM (ng m^{-3})			~~RGM~~GOM (pg m^{-3})			PBM (pg m^{-3})		
	Mean±σ	Range	N	Mean±σ	Range	N	Mean±σ	Range	N
Spring	3.89±1.79	0.2-21.3	7890	4.49±4.22	0.5-69.8	526	8.34±8.97	1.6-130.1	542
Summer	4.08±1.99	0.3-22.9	6050	3.66±4.39	0.5-45.2	511	3.61±4.38	0.5-41.9	570
Autumn	4.51±2.10	0.4-23.8	3632	5.65±8.93	0.5-78.9	274	59.9±153.5	0.5-1615	339
Winter	4.05±1.81	0.9-12.2	6381	2.59±2.58	0.5-9.5	541	56.1±134.9	0.5-1827	639
Total	4.07±1.91	0.2-23.8	23953	3.67±5.11	0.5-78.9	1852	30.02±100.3	0.5-1827	2090
Non-haze	3.95±1.93	0.2-23.8	20345	2.49±2.41	0.5-33.5	1508	23.3±90.76	0.5-1827	1708
Haze	4.74±1.62	2.1-16.5	3608	4.32±8.36	0.5-78.9	344	60.2±131.4	1.6-1615	382

带格式的：行距：1.5 倍行距

带格式的：中文(中国)

Table 2. Speciated atmospheric mercury concentrations in Hefei and other urban and rural areas.

Location	Classification	Time	TGM (ng m^{-3})	GEM (ng m^{-3})	~~RGM~~ GOM (pg m^{-3})	PBM (pg m^{-3})	Reference
Hefei	Suburb	Jul 2013-Jun 2014	4.1	4.07	3.67	30	This study
Hefei	Suburb	Feb-May 2009	2.53	-	-	-	Hu et al. (2014)
Beijing	Rural	Dec 2008-Nov 2009	3.23	3.22	10.1	98.2	Zhang et al. (2013)
Shanghai	Urban	Aug-Sep 2009	2.7	-	-	-	Friedli et al. (2011)
Nanjing	Urban	Jan-Dec 2011	7.9	-	-	-	Zhu et al. (2012)
Guiyang	Urban	Nov 2001-Nov 2002	8.4	-	-	-	Feng et al. (2004)
Guiyang	Urban	Aug-Dec 2009	-	9.72	35.7	368	Fu et al. (2011)
Changchun	Urban	Jul 1999-Jan 2000	18.4	-	-	276	Fang et al. (2004)
Changchun	Suburb	Jul 1999-Jan 2000	11.7	-	-	109	Fang et al. (2004)
Mt.Changbai	Remote	Aug 2005-Jul 2006	3.58	-	65	77	Wan et al. (2009a, b)
Mt.Gongga	Remote	May 2005-July 2006	3.98	-	6.2	30.7	Fu et al. (2008a, b)
Mt.Waliguan	Remote	Sep 2007-Aug 2008	1.98	-	7.4	19.4	Fu et al. (2012a)
Mt.Leigong	Remote	May 2008-May 2009	2.8	-	-	-	Fu et al. (2010)
Shangri-La	Remote	Nov 2009-Nov 2010	2.55	-	8.22	38.82	Zhang (2015)
Detroit, USA	Urban	Jan-Dec 2004	-	2.5	15.5	18.1	Liu et al. (2010)
Dexter, USA	Rural	Jan-Dec 2004	-	1.6	3.8	6.1	Liu et al. (2010)
Houston, USA	Urban	Aug-Oct 2006	-	1.66	6.9	2.5	Brooks et al. (2010)
Florida, USA	Urban	Jul 2009-Jul 2010		1.3	3	2	Peterson et al. (2012)
Maryland, USA	suburb	2007-2015		1.41	4.6	8.6	Ren et al. (2016)
Göteborg, Sweden	Urban	Feb-Mar 2005	-	1.96	2.53	12.5	Li et al. (2008)
Nova Scotia, Canada	Urban	Jan 2010- Dec 2011		1.67	2.07	2.32	Cheng et al. (2014)
Northern Hemisphere background value					1.5-1.7		Lindberg et al. (2007)

带格式的：中文(中国)

~~**Table 3.**~~

Table 3. Correlation coefficients and slopes between GEM concentration and CO concentration during atmospheric mercury pollution events.

Event	Start Time (UTC + 8 hr)	End Time (UTC + 8 hr)	Duration (h)	GEM (ng m^{-3})	CO (ppbv)	GEM/CO (slope, ng m^{-3} $ppbv^{-1}$)	R^2
1	2013/11/21 03:00	2013/11/22 02:00	23	8.37±2.42	4481.6±717.3	0.0018	0.29
2	2013/12/03 20:00	2013/12/04 09:00	13	7.51±0.67	5270.0±744.5	0.0001	0.02
3	2013/12/07 04:00	2013/12/09 04:00	48	9.21±1.16	5943.8±1394.1	0.0004	0.23
4	2013/12/19 09:00	2013/12/20 09:00	24	4.35±0.17	3907.6±353.0	0.0002	0.03
5	2013/12/24 19:00	2013/12/25 15:00	20	5.58±0.94	4930.8±919.7	0.0012	0.01
6	2014/01/17 22:00	2014/01/19 13:00	39	5.80±0.83	5746.3±1626.9	0.0003	0.28
7	2014/01/25 02:00	2014/01/25 22:00	20	6.03±0.50	8797.9±2244.3	0.0002	0.59
8	2014/03/16 05:00	2014/03/16 20:00	15	4.46±0.47	2261.7±440.2	0.0010	0.79
9	2014/03/17 06:00	2014/03/18 12:00	30	8.85±2.46	2697.1±590.3	0.0030	0.51
10	2014/05/21 00:00	2014/05/21 11:00	11	5.74±0.94	3676.7±1690.0	0.0050	0.79

Notes: these episodes were identified using the following criteria: (a) the duration of elevated GEM concentration lasted for >10h; (b) the selected hourly average GEM concentration higher than the seasonal average GEM concentration.

带格式的：中文(中国)

Table 4. The production of NO_2HgOH and d[NO_2HgOH]/dt at different NO_2 concentrations

NO2 (ppbv)	10	20	30	40	50	60	70	80	90	100
d(NO_2HgOH)/dt (molecule cm^{-3} s^{-1})	0.36	0.71	1.04	1.37	1.68	1.99	2.28	2.56	2.83	3.10
NO2HgOH (pg m^{-3}, 1hr)	0.56	1.10	1.63	2.13	2.61	3.08	3.54	3.97	4.40	4.81

带格式的：行距：1.5 倍行距

带格式的：两端对齐

带格式的：中文(中国)

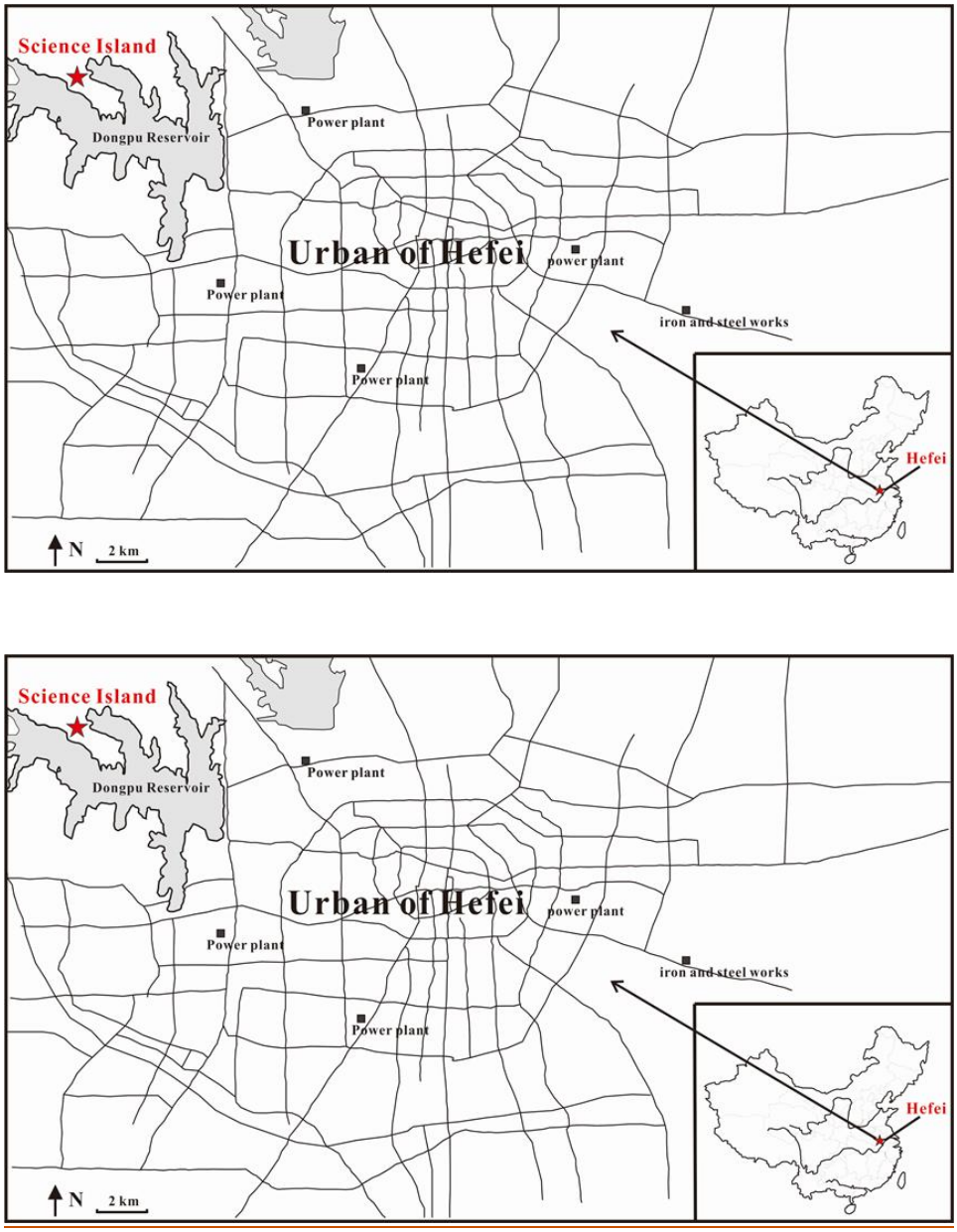

Fig. 1. Location of the ~~monitoring~~study site in Hefei, China.

带格式的：行距：单倍行距

带格式的：中文(中国)

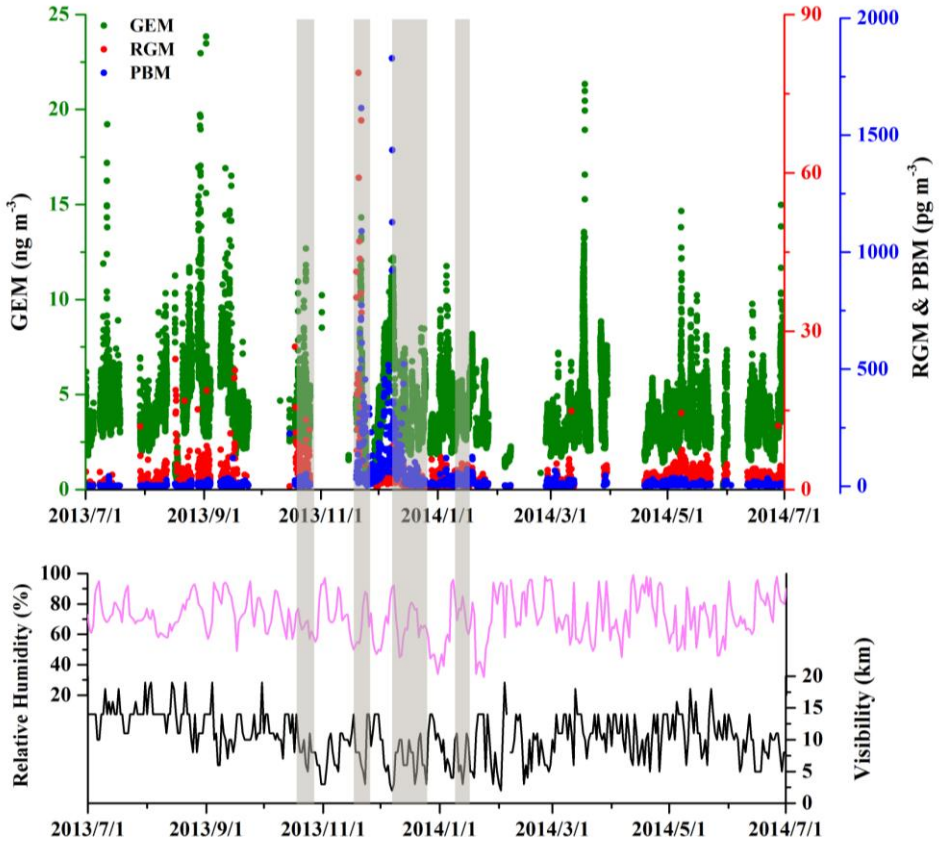

1321
1322

带格式的：中文(中国)

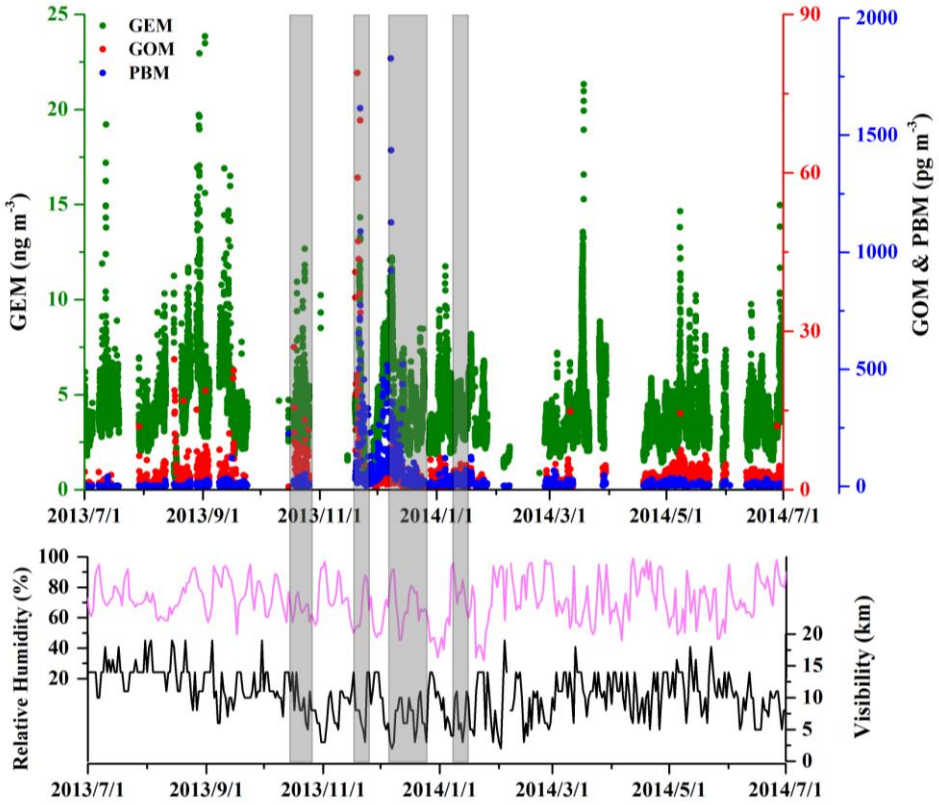

Fig. 2. Time series of GEM, ~~RGM~~GOM and PBM concentrations, along with visibility, relatively humidity, at the monitoring site in Hefei from July 2013 to June 2014. The GEM data were at a 5-min resolution, and the ~~RGM~~GOM and PBM data were two-hour averages. The gray columns show the major haze pollution episodes occurred during the study period.

带格式的：字体：加粗

带格式的：中文(中国)

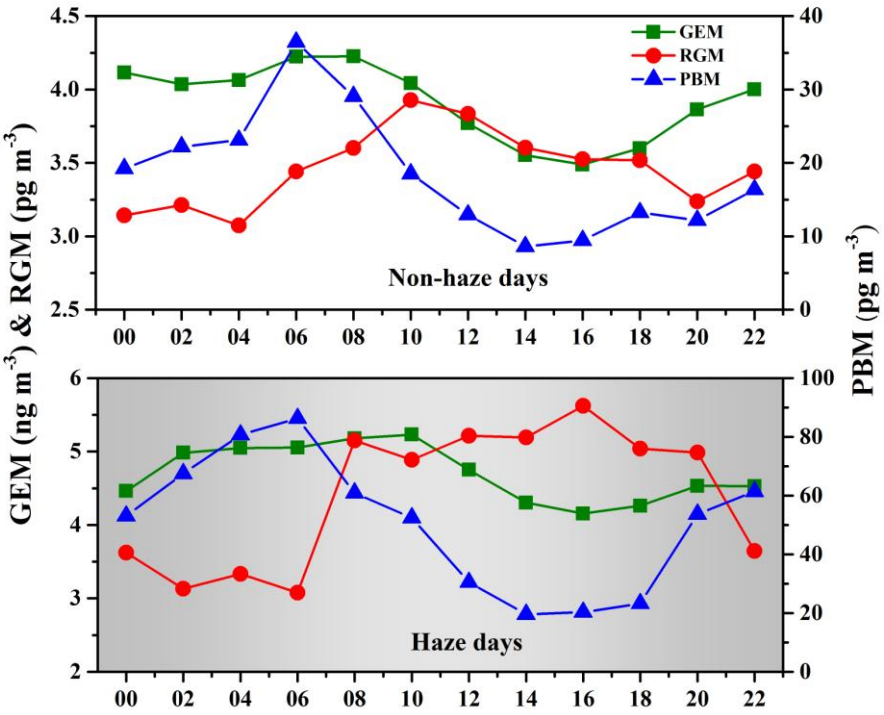

1330

1331

带格式的：中文(中国)

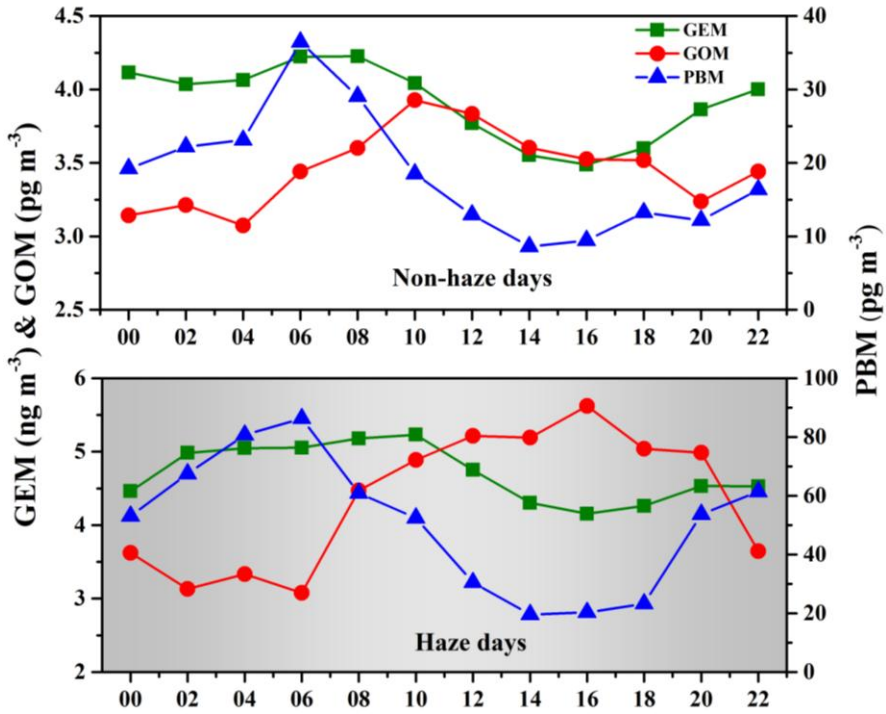

Fig. 3. Diurnal trends of GEM, ~~RGM~~GOM and PBM concentrations in Hefei during non-haze and haze days (Local time = UTC + 8 hr). The data were two-hour averages.

带格式的：中文(中国)

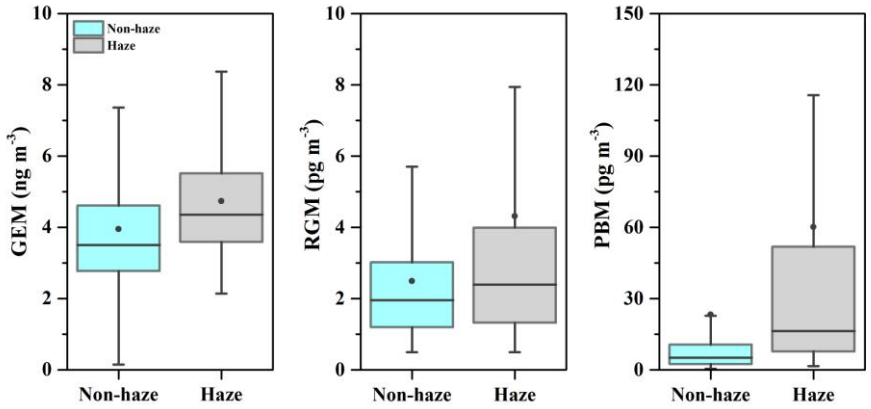

1336

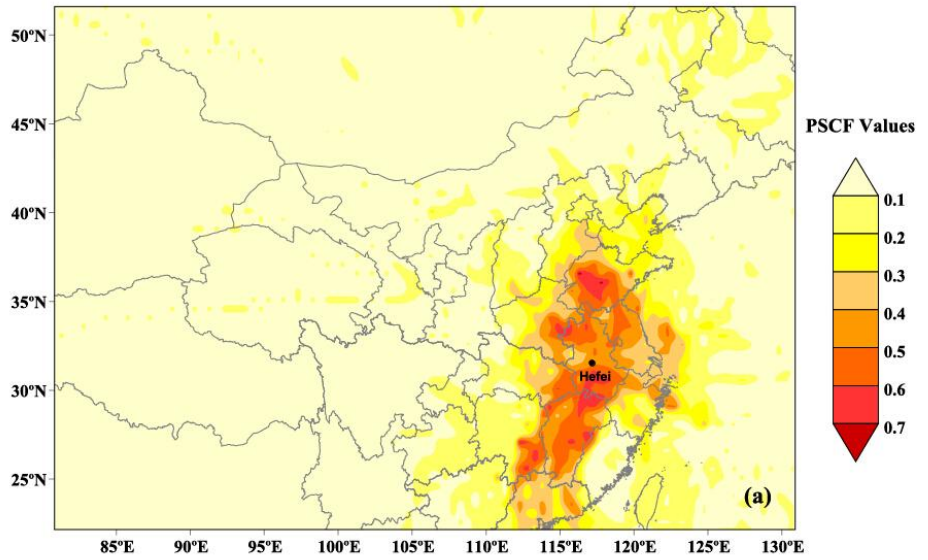

1337

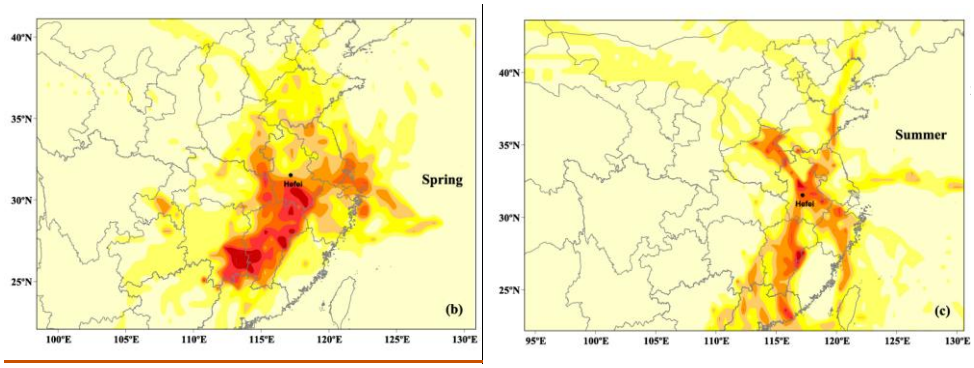

1338

带格式的：中文(中国)

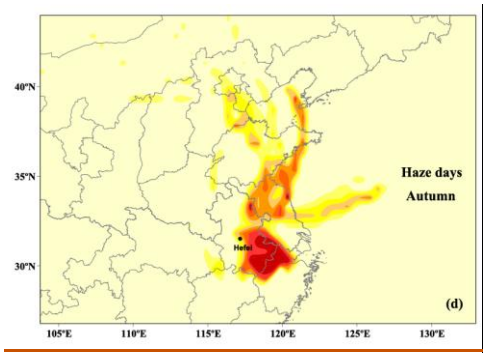

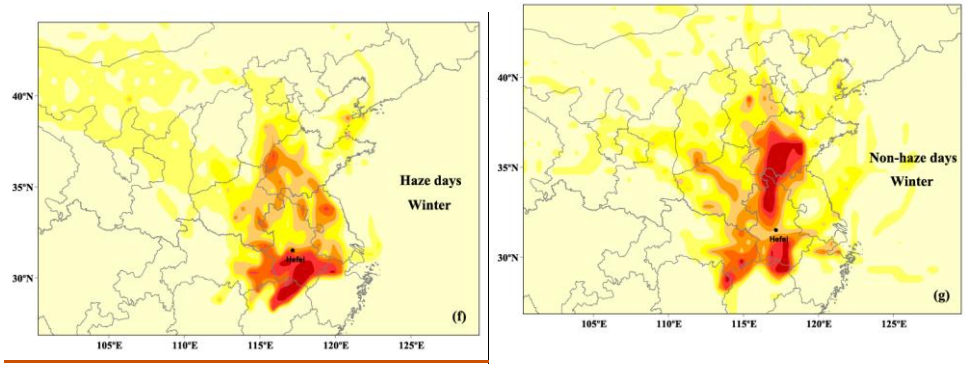

Fig. 4. ~~GEM, RGM and PBM concentrations during non-haze and haze days. The GEM data were at a 5-min resolution, the RGM and PBM data were two-hour averages.~~

带格式的：两端对齐

带格式的：字体颜色：红色

带格式的：中文(中国)

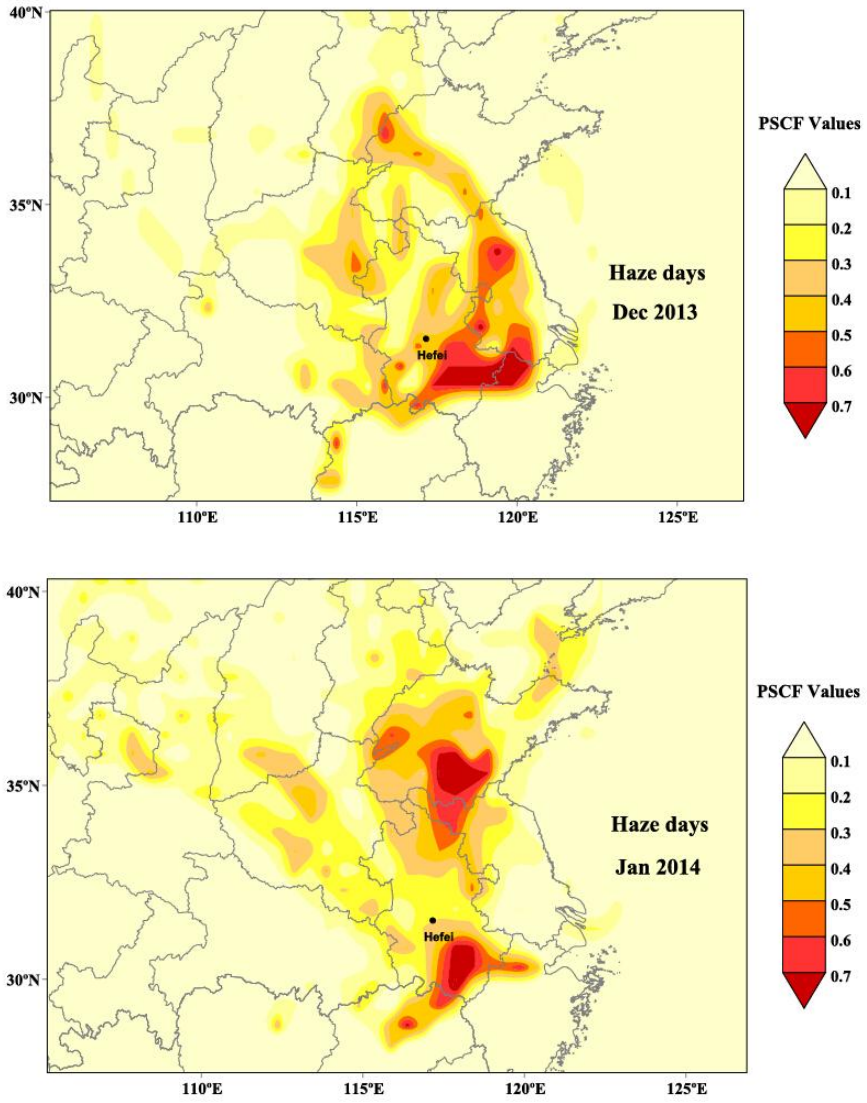

~~Fig. 5.~~ ~~Likely sources areas of GEM during haze days identified by PSCF analysis.~~

带格式的：中文(中国)

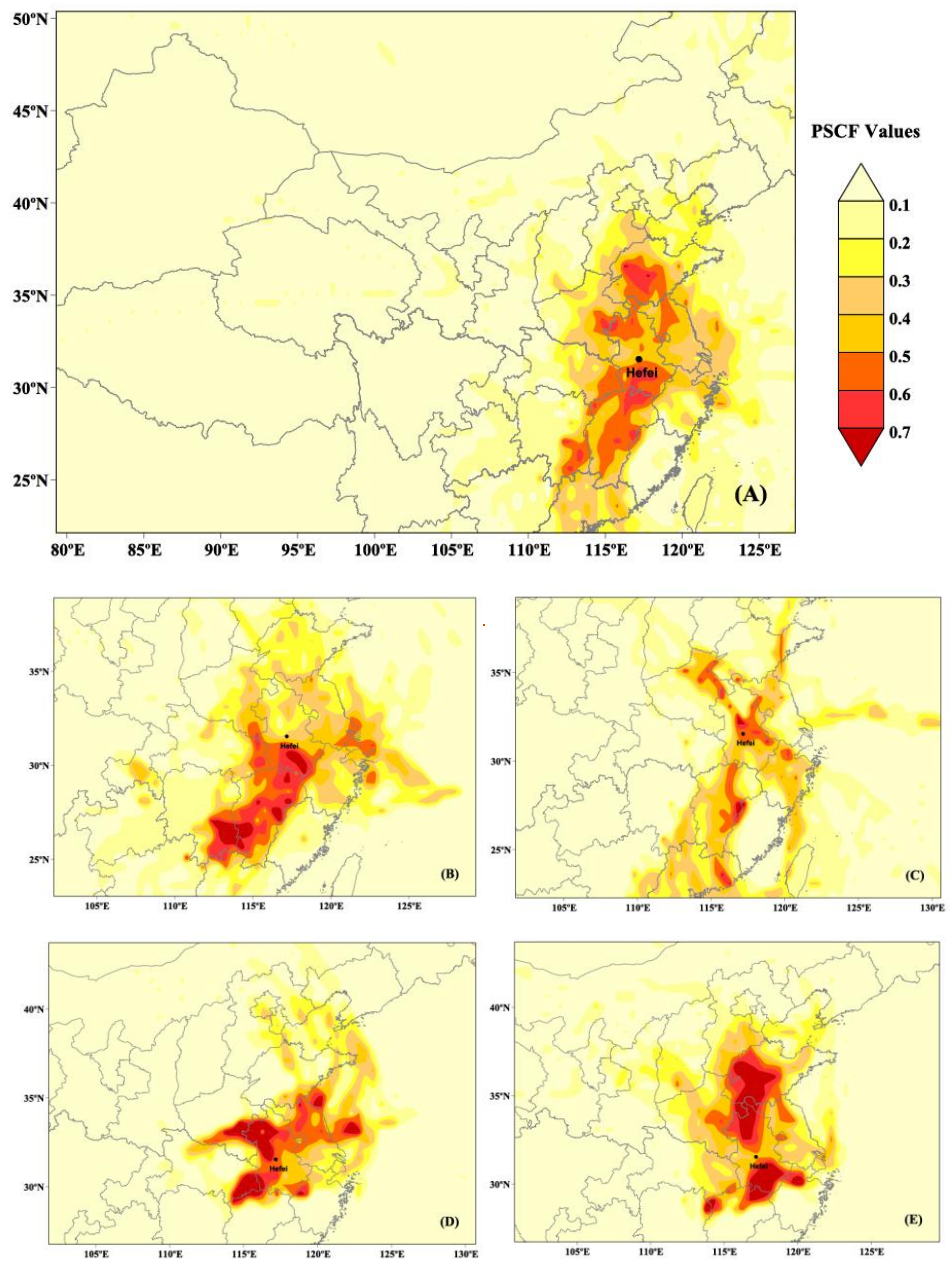

~~Fig. 6.~~ Likely emission ~~sources~~source areas of GEM simulated by PSCF analysis. (~~A~~a) overall (from July 2013 to June 2014), (~~B~~b) spring, (~~C~~c) summer, (~~D~~)d) haze days in autumn, (~~E~~)e) non-haze days in autumn, (f) haze days in winter~~.~~, (g) non-haze days in winter.

带格式的：字体颜色：红色
带格式的：字体颜色：红色
带格式的：字体颜色：红色
带格式的：字体颜色：红色
带格式的：字体颜色：红色
带格式的：字体颜色：红色
带格式的：字体颜色：红色
带格式的：字体颜色：红色
带格式的：中文(中国)

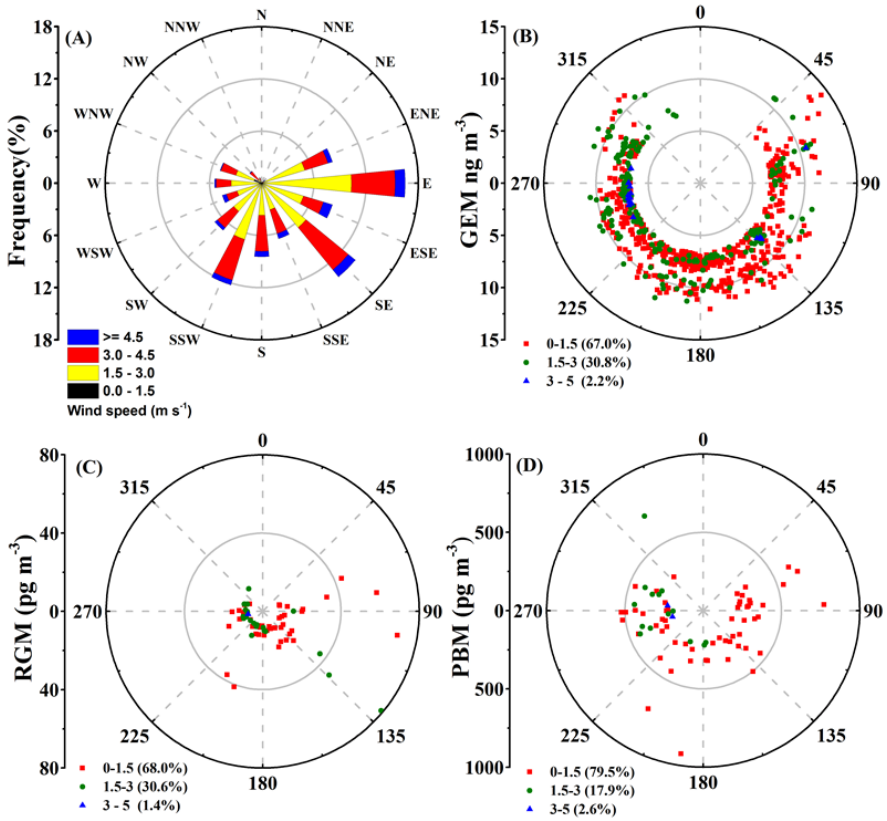

1371

带格式的：中文(中国)

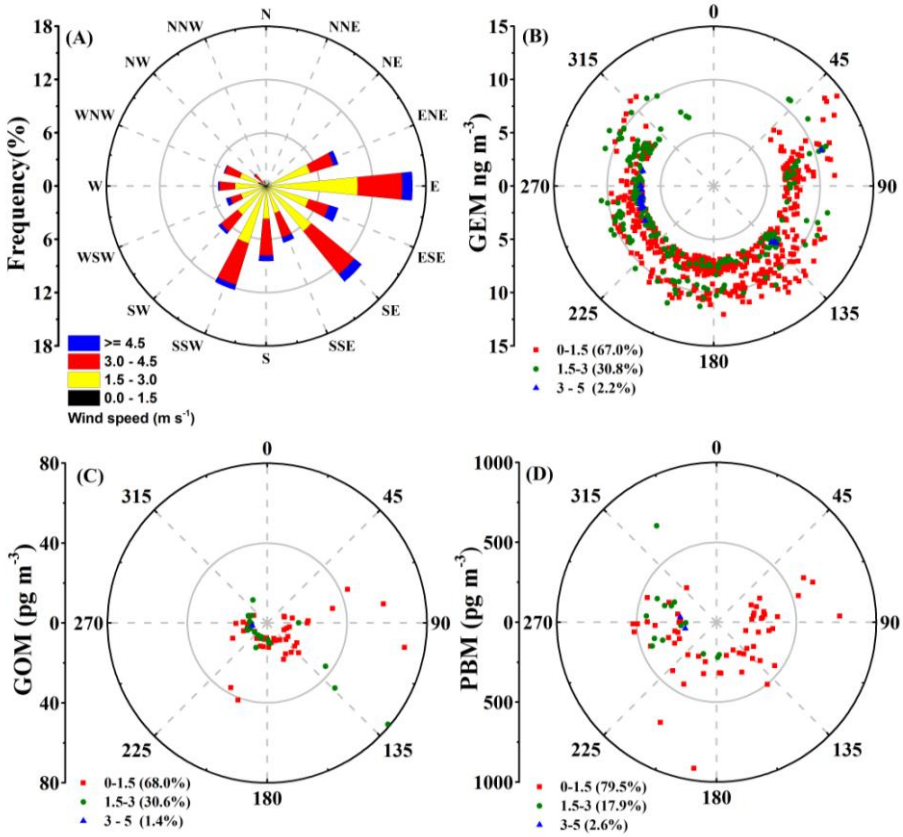

Fig. ~~75~~. Wind direction and speed at the Science Island Meteorological Station during the study period. (A) the wind rose for the whole study period; (B), (C) and (D) are the wind rose diagrams for GEM, ~~RGM~~GOM and PBM concentrations above the 90th percentile values, respectively.

带格式的：居中，行距：单倍行距

带格式的：中文(中国)

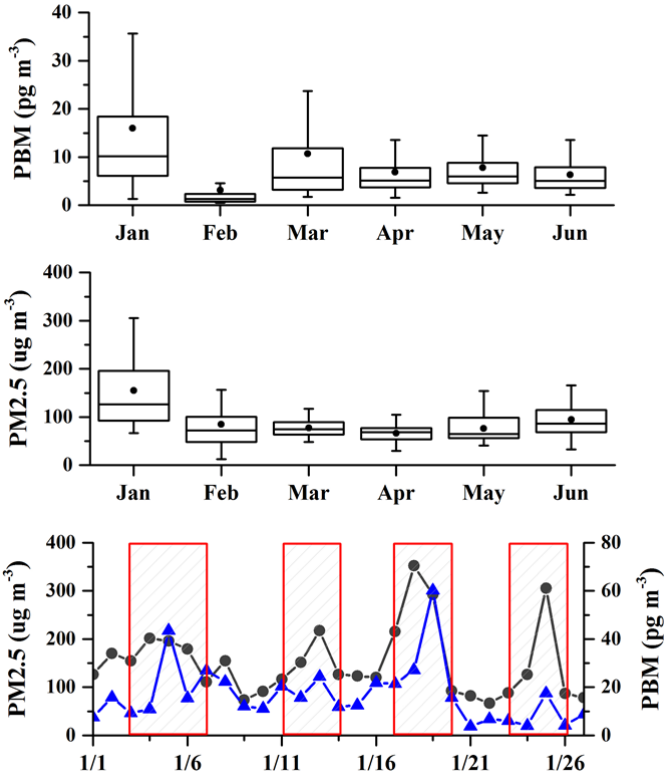
PBM (pg m-3)
40
30
20
10
0
Jan
Feb
Mar
Apr
May
Jun
PM2.5 (ug m-3)
400
300
200
100
0
Jan
Feb
Mar
Apr
May
Jun
PM2.5 (ug m-3)
400
300
200
100
0
80
60
40
20
0
PBM (pg m-3)
1/1
1/6
1/11
1/16
1/21
1/26

带格式的：中文(中国)

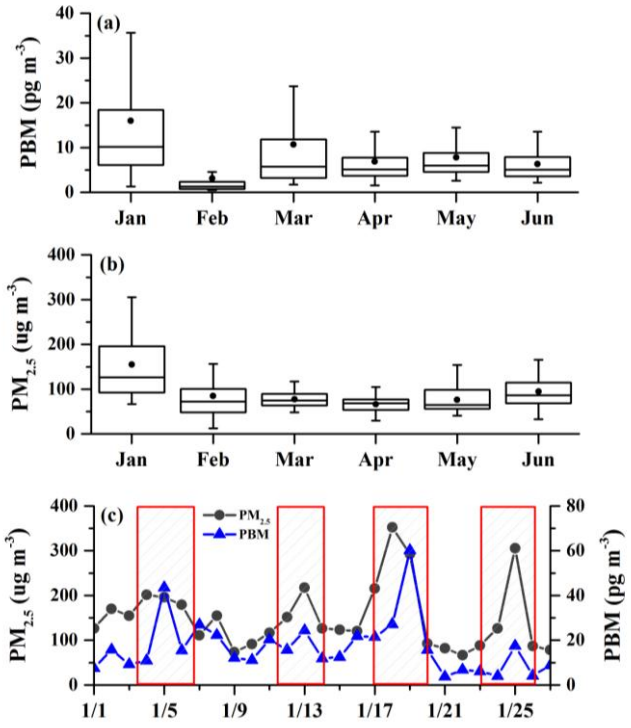

Fig. ~~8.~~ 6. Monthly variation of (a) PBM and (b) $PM_{2.5}$ concentrations from January to June, 2014~~.~~, (c) average daily $PM_{2.5}$ and PBM concentrations in January, 2014.

带格式的：字体颜色：红色
带格式的：字体颜色：红色
带格式的：字体颜色：红色
带格式的：左
带格式的：字体颜色：红色，下标
带格式的：字体颜色：红色
带格式的：字体：加粗，字体颜色：红色

带格式的：中文(中国)

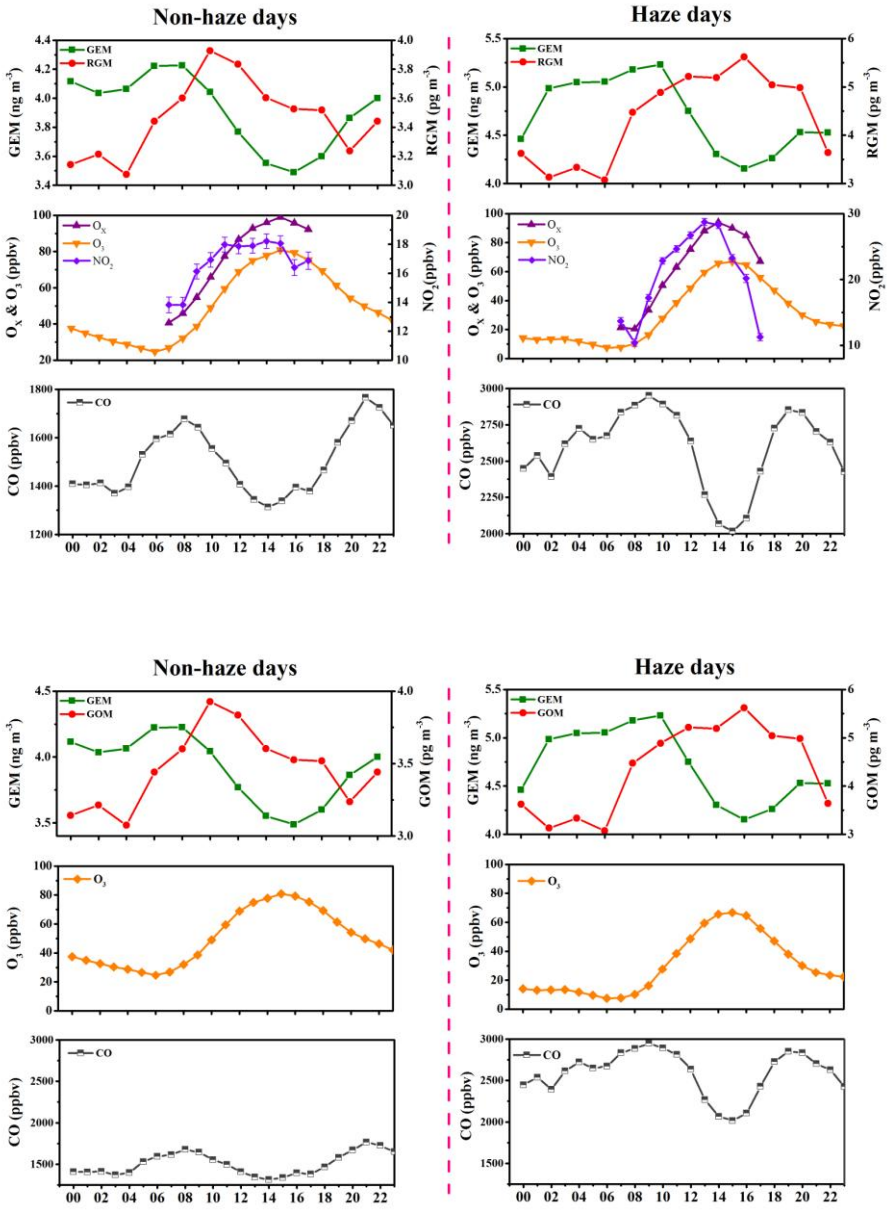

Fig. ~~9.~~7. Diurnal variations of GEM, ~~RGM and Gas Phase Data (O_X,~~ GOM, O_3, ~~NO_2~~ and ~~CO)~~ concentrations during non-haze and haze days. ~~Notes:~~

带格式的：字体颜色：红色

带格式的：字体颜色：红色

带格式的：字体颜色：红色

带格式的：字体颜色：红色

带格式的：字体颜色：红色

带格式的：中文(中国)

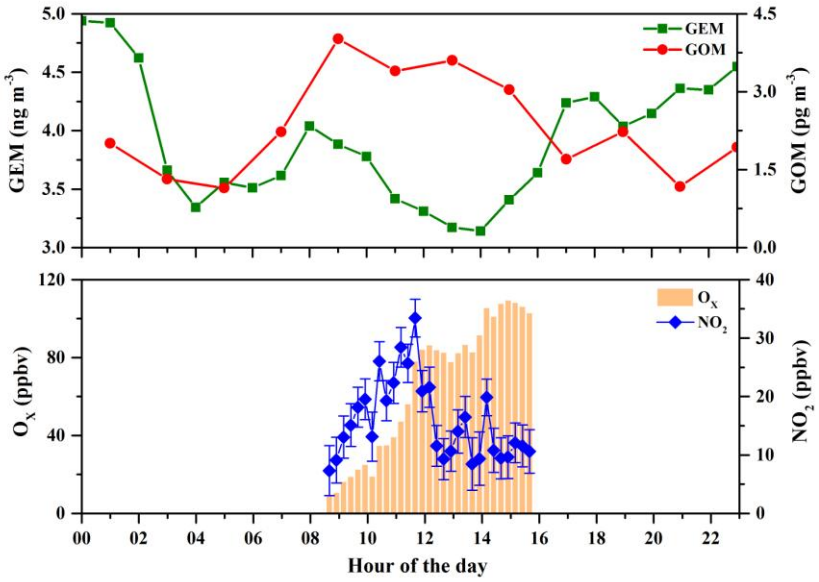

Fig. 8. A case study of diurnal variations of GEM, GOM, O_X, and NO_2 at Hefei (20th November, 2013). The top panel shows the hourly averaged GEM and GOM concentrations, and the bottom ~~is the carbon monoxide mixing ratio. Middle are the averaged O_3,~~ panel shows the O_X (O_X= NO_2 +O_3) and the NO_2 concentrations. ~~Top are the hourly averaged GEM and RGM concentrations. The~~ The error bars for NO_2 refer to the NO_2 standard ~~deviations~~errors.

带格式的：字体颜色：红色
带格式的：字体颜色：红色
带格式的：字体颜色：红色
带格式的：字体颜色：红色
带格式的：字体颜色：红色
带格式的：字体颜色：红色
带格式的：两端对齐，行距：1.5 倍行距

带格式的：中文(中国)